Dear editor,

In this revised version, we addressed all comments from the reviewers. We modified some expressions and added more explanations to our methods and results, as requested by the reviewers. We also modified the discussions on the uncertainty of the quantification of runoff components in this manuscript. Some tables and figures were modified in response to the reviewers' comments. We renamed all the mixing approaches in this revised version. In particular, the traditional end-member mixing approach was abbreviated as EMMA. The Bayesian approaches considering the correlation between $\delta^{18}O$ and $\delta^{2}H$ were renamed as Bayesian_3_OHcor (for three runoff components) and Bayesian_4_OHcor (for four runoff components). Bayesian_3_OHind and Bayesian_4_OHind were used to name the Bayesian approaches assuming $\delta^{18}O$ and $\delta^{2}H$ are independent from each other. The Bayesian approaches considering the isotope fractionation during the mixing process were renamed as Bayesian_3_OHcor_Frac and Bayesian_4_OHcor_Frac.

Changes from the original manuscript were labeled in the following change marks version. We thank the three reviewers for their constructive comments, which are extremely helpful for the improvement of this paper. Also, we are much appreciated for your handling of the review of this paper.

Sincerely,

Zhihua He
zhh624@mail.usask.ca

Reviewer 1:

1. Summary: This paper provides an interesting comparison of traditional end-member mixing analysis approaches versus Bayesian statistical approaches for estimating contributions of different runoff components in a glacierized basin in Central Asia. The paper provides an interesting in-depth analysis of the effect of different sources of uncertainty on the Bayesian modeling results. The results clearly highlight that the Bayesian approaches predict more or less the same runoff contributions as the EMMA model when both models have a large sample size, but the Bayesian approach reaches a much smaller uncertainty that is about 50-60% of the EMMA approach. The results further show that the Bayesian approach is superior to the EMMA approach in situations where sample numbers are low and end members look very similar (e.g. snow and glacier melt signature is similar). The results further show that explicitly considering the correlation between ^{2}H and ^{18}O in the mixing model, further reduces the uncertainty in the results. The paper is well motivated, and the introduction provides a comprehensive overview of the current research on isotope hydrograph separation of runoff components in glacierized basins. The authors explain well the limitations of existing "traditional" approaches such as end-member-mixing-analysis and describe clearly the advantages that Bayesian approaches provide to this problem. My only recommendation would be to add a figure showing the time series of the isotope and EC data and to clarify the "fractionation effect" in the methods and results section. It is currently not clear what this Bayesian modeling scenario encompasses and because of that the section that describes the results of this scenario analysis is confusing. Other than that, the paper, overall, is well written and easy to comprehend. The authors made all relevant code available.

Reply: Thanks for your positive comments on this paper. We have addressed all your concerns in the revised manuscript. A figure has been added to the supplement to show the time series of water isotope and EC data along with temperature, precipitation and streamflow data. The fractionation effect has been explained in more details, and the related expressions have been refined to reduce confusion.

2. Line 146: Please specify what "pure plastic bottles" are? Typically, we state the type (e.g. HDPE or glass) and size of the bottle used to sample water.

Reply: We specified the bottles as 50 ml high-density polyethylene (HDPE) bottles in the revised manuscript.

3. Line 108: Please be more specific. What do you mean by "water sampling uncertainty" here? Do you mean the uncertainty associated with having just a few samples?

Reply: Specified this as "water sampling uncertainty associated with the representativeness of the water samples caused by the limited sample site and sample size". See lines 120-121.

4. Line 159: What is the size of the Golubin glacier in the watershed? You mention that glaciers cover about 17% of the watershed. What is the fraction that the Golubin glacier represents in the 17%? What is the streamflow (volume) contribution of the glacier to the entire basin? Is the Golubin glacier representative of the elevation range and snow accumulation of the other glacierized areas in the basin? Did you take grab samples from the other glaciers for comparison? I am a bit concerned that the glacier melt contribution of the Golubin glacier is too small to really make a difference isotopically.

Reply: The Golubin glacier has an area of ~5.7 km^2 and extends over an elevation range from 3232 to 4458 m a.s.l.. The elevation range of the entire glacierized area extends from 3218 to 4857 m a.s.l., with about 76% located between 3700 and 4100m a.s.l.. Both the elevation range and the mean elevation (3869 m a.s.l.) of the Golubin glacier are close to those of the entire glacierized area (mean elevation is 3945m a.s.l.). The Golubin glacier represents about 14.4% of the entire glacierized area, while its elevation range covers around 95.6% of the entire glacier range. We only collected meltwater samples from the Golubin glacier, due to the logistic limitations in the remaining glacierized area. Considering the isotopic compositions of snow and glacier meltwater are particularly dependent on the elevation of glacierized area, the sampled meltwater from the Golubin glacier could represent meltwater originated from the primary melting locations in the entire glacierized area. We added these explains in the revised manuscript. See lines 146-150 and 617-622.

5. Line 177: Please specify the model and manufacturer of the pH, EC and TDS meter used in this study. Please indicate the precision that this instrument can achieve.

Reply: Specified as "We used the Hanan Instruments HI-9813 PH EC/TDS portable meter to measure the EC values of water samples, with a measurement precision of 0.1 µs/cm". TDS and pH values of water sample were not recorded. See lines 209-210.

6. Line 178: How did you determine what constitutes an "abnormal isotopic compositions"? Please describe the method/approach you used.

Reply: We used threshold values to identify abnormal values of $\delta^{18}O$ and EC located far away from the sample clusters. For $\delta^{18}O$, sample values higher than 5‰ were excluded. For EC, *sample values higher than 210 μs/cm were excluded*. *We specified that in the revised manuscript. See lines 214-216.*

7. Line 185: It would be helpful if the authors could add text on how much rainfall and streamflow the Ala-Archa basin typically gets and what the mean annual temperature is. In addition, I would like to suggest providing a graph of the temperature, precipitation and streamflow observed in the Ala-Archa basin between 2012 and 2017 so that the reader can evaluate the interannual variability in the hydro-climate. Since the authors decided to average isotope and EC values across 5 years of observations, this information might help explaining some of the uncertainty in the data.

Reply: A figure for the daily precipitation, temperature and streamflow measured at the basin outlet during 2012-2017 has been added in the supplement (also see the following Figs. S1c-e). Related sentences have been added to describe the hydro-climate data: "The annual mean precipitation and temperature measured at the Baitik meteorological station during 2012-2017 are 538 mm yr^{-1} and 7.2 ℃, respectively. The mean daily streamflow during 2012-2017 is about 6.3 m^3/s." The CRC estimated by the mixing approaches refer to the mean contributions in each of the three seasons during the period of 2012-2017. See lines 150-152 and 222.

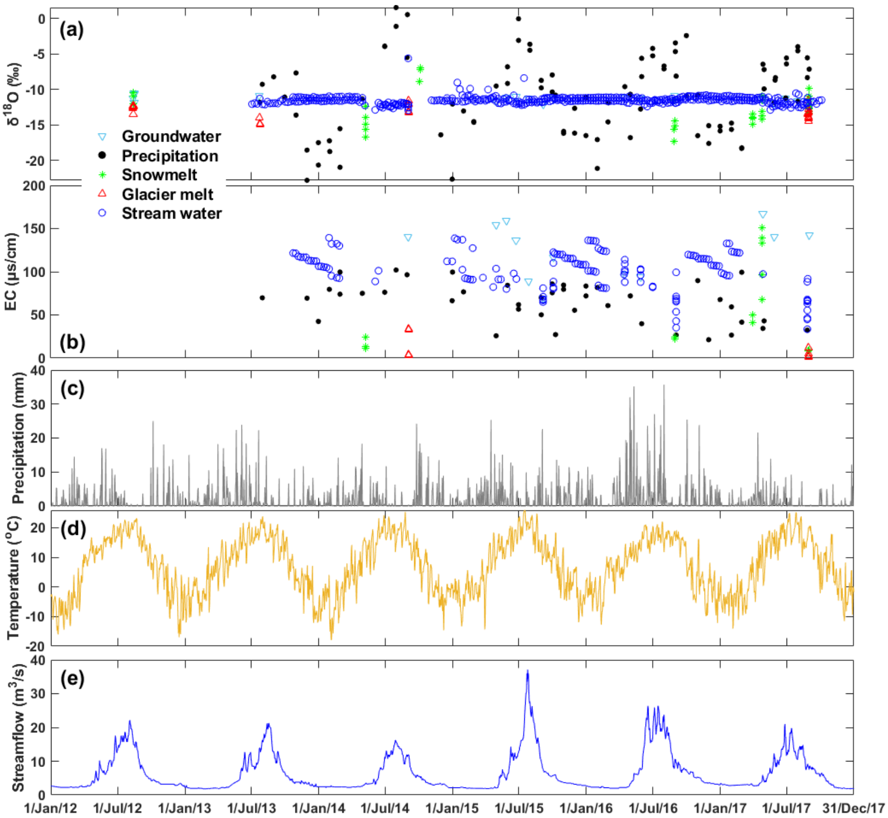

Figure S1. (a)-(b) Tracer signatures of water samples during the sample period of 2012-2017;(c)-(d) Daily precipitation and temperature measured at the Baitik meteorological station in 2012-12017; (e) Daily streamflow measured at the Ala-Archa hydrologic station during 2012-2017.

8. Line 185: Please add a time series graphs of your isotope and EC, pH and TDS measurements. This graph does not have to be in the main text but could be provided as supplemental material so that the reader can see how the collected data looks like.

Reply: Please, see the last response. The pH and TDS data were not recorded.

9. Line 250: Please show the histograms of the isotope and EC data. The Bayesian approach assumes that the data is normally distributed, however, based on the data range shown in Figure 3, it looks like that some data might not have been normally distributed? You could report results from a normality test to be sure.

Reply: Figure 3 only shows the maximum and minimum tracer signatures of each water source. It is not related to the distributions of measured water tracers. The histograms of isotope and EC data in the glacier melt season have been presented in Fig. 5 in the manuscript. A Kolmogorov-Smirnov test has been carried out for both isotope and EC tracers of all water sources. The tracer data of runoff components (i.e., rainfall, snowmelt, groundwater and glacier melt) generally pass the normal distribution test at significance levels of p-values > 0.3, while the tracer data of stream water fail to pass the normal distributions test partly caused by the extreme isotope and EC values. The EC data of glacier melt also fail to pass the normal distribution test, which can be caused by the low sample size. We thus assume the prior distributions of tracers of runoff components are normal in Eqs. 6-8. The prior distributions of tracers of stream water are first assumed as normal in Eqs. 6a and 8a, and the mean tracer signatures are then calculated by the mixing of tracers of runoff components in Eq. 9. We reported the test results in the revised manuscript. See lines 282-288.

10. Line 300: It is not quite clear what you mean by "the fractionation effect". Could you be more specific and clarify to the reader when, where this fractionation effect might occur and how it could impact the observed values?

Reply: The water sources for runoff, such as rainfall and meltwater, are subject to evaporation before reaching the basin outlet, especially in summer. However, the isotopic composition of stream water was measured at the basin outlet, and the contributions of runoff components are quantified for the total runoff at the basin outlet. After the long routing path from the sampled sites to the basin outlet, the isotopic compositions of rainfall and meltwater mixing at the basin outlet could be different from those measured at the sampled sites, caused by the evaporation fractionation effect. The isotopic composition of water sources at the sample sites are assumed to be normally distributed in Eqs. 6-7, and the changes in the isotopic compositions of water sources caused by the evaporation fractionation effect are represented by the modification variables $\xi^{18}O$ and $\xi^{2}H$ *in Eq. 10. The evaporation fractionation has no effects on the observed isotopic compositions, but does have one on the quantification of runoff components, which is considered as a source of model uncertainty in the study. We added a more detailed explanation for that in the revised manuscript. See lines 377-392.*

11. Line 435: The results section on the fractionation effect is confusing. This is mainly because it is not clear what the fractionation effect is and how it is estimated in the sample groups. I would recommend clarifying this in the methods.

Reply: Please, see the last response. We added a more detailed explanation in the method section. See lines 383-392. The quantification of runoff components in two Bayesian scenarios are compared. In the first scenario (using Bayesian_3_OHcor and Bayesain_4_OHcor), the fractionation effect on isotopic compositions of water sources are ignored, i.e., the isotopic compositions of water sources at the basin outlet are assumed as same as those measured from the sample sites. In the second scenario (using Bayesian_3_OHcor_Frac and Bayesian_4_OHcor_Frac), the evaporation fractionation effect on the isotopic compositions of water sources have been considered. The mixing of water tracers of stream water are represented by Eq. 10. Figure 9 illustrates the effects of fractionation on the quantification of runoff components in all three seasons. The estimated changes in $\delta^{18}O$ of each water source are presented in Figs. 9a-c, and the contributions of runoff components quantified by the two scenarios are compared in Figs. 9d-f.

12. Line 463: I would suggest rephrasing to: "The TEMMA estimated similar CRCs for most mixing models but at a larger uncertainty than the Bayesian approaches."

Reply: Done. Thanks.

13. Figure 3: During the glacier melt season the snowmelt end member has a much lower EC value than what was estimated for the cold and snowmelt seasons. Can you explain why the EC is all the sudden so much lower? Since it is most likely not fresh snow that is melting during the glacier melt season, this trend is somewhat surprising.

Reply: In the cold and snowmelt seasons, some snowmelt samples also have EC values as low as those in the glacier melt season (see Fig. 3). The snow samples in the glacier melt season were only collected from the accumulation zone of the glacier, thus resulting in small variability in the EC values. The snowpack in the accumulation zone is accumulated by fresh snow in the snow period (summer type accumulation glacier).This leads to low EC values in the snowmelt samples. We added this discussion in the revised manuscript. See lines 432-437.

14. Minor comments: Line 43: Should be "led" instead of "leaded". Line 114: Use "of" instead of "for the". Line 124: Should be "glaciers cover" instead of "glacier covers" unless you only have one glacier: : : Line 127: Should be "shows". Line 129: Word missing. Please insert "runoff" after "generates". Line 138: Should be "since the 1960s". Line 158: Should be "was" instead of "were". Line 162: Suggest using "from early March". Line 163: Suggest using "due to" instead of "caused by". Line 168: Please add "meltwater samples". Line 172: "at Helmholtz" Line 183: "split" would be a better word than "distributed". Line 292: please delete "keeping". Line 309: Language! Please rephrase the second part of this sentence. Line 469: Replace "occasionally" with "sporadically". Line

499: Replace "though" with "despite". Line 520: replace "spring points" with "springs".

Figure 1: Please remove the underscore for the Rain collector label in the legend.

Reply: All done. Thanks.

<u>**Reviewer 2:**</u>

1. This is a very interesting and well written manuscript that compares the traditional tracer-based end-member mixing model approach with different versions of a Bayesian mixing model to quantify water sources to runoff in a glacierized catchment in Kyrgyzstan. The findings of this work may have practical implications when applying these approaches to other catchments and are therefore surely interesting to the readers of HESS. The manuscript is logically organized, it is nicely illustrated, the interpretation is well supported by the data, and the discussion is coherent and with relevant and updated references. However, there are some moderate and minor issues that need to be clarified and that I invite the Authors to consider. Please, find these comments, suggestions, and a few corrections in the attached annotated manuscript. I hope they can be useful to the Authors to improve their work.

Reply: Thanks a lot for the positive comments. We have addressed all your concerns in this revised manuscript.

2. Lines 29 and 143: 'water tracer' to 'tracers' or 'hydrological tracers'; line 38: 'were' to 'was'; line 181: 'clod' to 'cold'; line 418: 'show' to 'shows'; line 490: 'rely' to 'relies'; line 726: Change the sentence into "CV stands for coefficient of variation"; line 734: 'snowmlet' to 'snowmelt'.

Reply: All done, thanks.

3. Lines 37 and 57: No need to make up a new acronym 'TEMMA'. EMMA is enough, there is no risk to confound it with the other approach.

Reply: The traditional end-member mixing approach is renamed as EMMA.

4. Line 70: These are sources of uncertainty that are important in any catchment, not necessarily glacierized catchments. Please, specify why the latter are particularly prone to difficult application of HS (e.g., multiple water sources, high spatio-temporal variability of water sources etc.).

Reply: The glacierized catchments are challenging for application of the end-member mixing approaches because of the following reasons: (1) The catchment elevation generally extends over a large range, leading to strong spatial variability in climate forcing (precipitation and temperature) and the tracer signatures of water sources; (2) The number of end-member water sources for runoff is high, additionally including snow and glacier meltwater; (3) Water sampling in high-elevation glacierized catchment is difficult due to the logistical limitations, *resulting in small sample sizes for the application of EMMA. We specified these in the revised manuscript. See lines 67-73.*

5. Line 77: But only the statistical uncertainty! Please, specify.

Reply: Specified as the "statistical uncertainty" in this manuscript.

6. Lines 83-87: This two issues are important but not very clearly explain. Please, clarify.

Reply: We refined these sentences as follows: These include (1) inappropriate estimation of the variability of tracer signatures of water sources when only few water samples are available. The used Sd values of the measured tracer signatures likely fail to represent the variability of water tracer signature of individual water source across the basin, due to the small water sample sizes; (2) The correlation of tracer signatures and runoff components are inevitably ignored, due to the assumption of independence of the multiple uncertainty sources. The correlation between $\delta^{18}O$ and $\delta^{2}H$ of each water source, as well as the interaction between runoff components could provide additional constraints on the uncertainty in the quantification of runoff components, which however are typically ignored in the Gaussian error propagation technique. See lines 88-97.

7. Line 93: In this paragraph it's important, in my opinion, to add a description on how uncertainty is treated in the Bayesian approach. This is particularly important for the research question #2.

Reply: In the Bayesian approach, both the statistical and model uncertainty are represented by the posterior distributions of parameters. The parameter uncertainty is estimated based on likelihood observations using a Markov Chain Monte Carlo procedure. This explanation has been added in the revised manuscript. See lines 106-109.

8. Line 109: How do Bayesian mixing models estimate the isotopic fractionation? I suggest to add a sentence here.

Reply: Modified as "Benefiting from the prior assumptions for changes in isotope signatures during the mixing process, the Bayesian approach bears the potential to estimate the fractionation effect on isotopic signatures, which however, has not been investigated either." See lines 122-124.

9. Line 113: In the two research questions outlined here it is not adequately stressed/explained why a glacierized catchment has been chosen for addressing these questions. Indeed, they can be applied to any catchment. Please, specify this.

Reply: We added a more detailed explanation here: "In Central Asia, glacierized catchments provide important fresh water supply for downstream cities and irrigated agriculture. Quantifying the contributions of multiple runoff components to total runoff is important for *understanding the dynamics of water resource availability at the regional scale. However, uncertainty in the quantification of runoff components in the glacierized catchments are particularly large because of the following reasons: (1) The catchment elevation generally extends over a large range, leading to strong spatial variability in climate forces (precipitation and temperature) and the tracer signatures of water sources; (2) The number of end-member water sources is large, additionally including snow and glacier meltwater; (3)Water sampling in high-elevation glacierized catchments is difficult due to the logistical limitations, resulting in small sample sizes to represent the tracer signatures of water sources." See lines 127-131.*

10. Line 143: As we know, EC is not as conservative as tracers. However, due to its easy use it has been often applied in catchment studies. Please, include a short discussion on the possible issue related to the lack of conservative behaviour (e.g., not so relevant at the catchmen scale, or at the runoff event scale etc.)

Reply: We added related discussion on this issue as follows: "EC data has been widely used for hydrograph separation, due to its easy use and quick measurement. While EC is not a conservative tracer, this may have only small effects on the application of hydrograph separation at the catchment scale." See lines 210-213.

11. Line 175: Any procedure to minimize memory effect (carry over effect) was performed?

Reply: Added: "A regular re-calibration procedure has been carried out for the isotope analysis." See line 206.

12. Line 176: First time it's mentioned...define electrical conductivity.

Reply: Defined on line 61.

13. Line 177: Can you quantify the term "abnormal"?

Reply: We used threshold values to identify abnormal values of $\delta^{18}O$ and EC located far away from the sample clusters. For $\delta^{18}O$, sample values higher than 5‰ were excluded. For EC, sample values higher than 210 µs/cm were excluded. We specified that in the revised manuscript. See lines 214-217.

14. Line 227: It's not clear to me how 4-component HS can be performed using two tracers only. Indeed, due to the collinearity of 18oxygen and deuterium, these two tracers cannot be treated independently. So, how are mixing approaches TEMMA4, Bay4 and Bay4cor defined? Please, this parts need to be extremely clear to the readers.

Reply: Yes, the values of $\delta^{18}O$ and $\delta^{2}H$ are typically correlated for each water source. However, the coefficients representing the correlation between $\delta^{18}O$ and $\delta^{2}H$ vary among the water sources in glacierized catchment (see Fig. 2), thus providing a basis for the EMMA_4 to quantify four runoff components. When quantifying four runoff components using three tracers, *four conservative equations for $\delta^{18}O$, $\delta^{2}H$, EC, and water volume are used (similar to Eq.1). The contributions of runoff components (**f**), as well as the partial derivatives used to calculate the uncertainty are solved from the four conservative equations using Matlab. However, the solutions are too lengthy to show in the text. As expected, results in Table 4 show that the EMMA_4 failed to distinguish snowmelt and glacier melt runoff, due to the similar tracer signatures of these two runoff components, but succeeded in quantifying the contributions of rainfall and groundwater. The Bayesian_4_OHind and Bayesian_4_OHcor estimated the contributions of four runoff components based on the prior distributions of $\delta^{18}O$, $\delta^{2}H$ and EC. The correlation between $\delta^{18}O$ and $\delta^{2}H$ is ignored in Bayesian_4_OHind. We used independent prior distributions for $\delta^{18}O$ and $\delta^{2}H$ of each water source. In Bayesian_4_OHcor, parameters describing the correlation between $\delta^{18}O$ and $\delta^{2}H$ of each water source were estimated by likelihood observations of the corresponding water source, which also vary among the water sources, thus providing a basis for the quantification of four runoff components using four mixing equations of tracer signatures (similar to Eq.9). The four-components approaches are developed in our study to investigate the following two questions: (1) Is the EMMA able to quantify four runoff components just using $\delta^{18}O$, $\delta^{2}H$, and EC? (2) Does the correlation between $\delta^{18}O$ and $\delta^{2}H$ help to reduce the uncertainty in the quantification of runoff components? We added these explains in the revised manuscript. See lines 266-273 and 336-344.*

15. Line 288: The three scenarios are not immediately clear. Does the mean refer to the spatial value or the temporal value, or the spatial-temporal value? The same question applies to sd. Then, different compared to what? Please, specify.

Reply: Meltwater sampling in glacierized catchments is typically difficult due to the logistic limitations. Thus, a small number of samples from a few sites are usually used for hydrograph separation. The uncertainty in the representativeness of meltwater samples implies an additional uncertainty source for quantification of runoff components. To investigate the effects of this type of sampling uncertainty, we set up three virtual sampling scenarios. Scenario I is used to evaluate the effects of meltwater sample size, in which four groups of meltwater sample are tested. The four sample groups have the same mean value and Sd of $\delta^{18}O$ or EC, but different sample sizes. Mean and Sd values of $\delta^{18}O$ or EC are calculated for all used meltwater samples in each group, referring to the spatio-temporal variability (same in the following two scenarios). Scenario II is used to evaluate the effects of sampled mean value of $\delta^{18}O$ (or EC) of meltwater. The four sample groups have the same sample size and Sd, but different mean values. Scenario III is used to investigate the effects of Sd values of sampled $\delta^{18}O$ (or EC). The four sample *groups have the same sample size and mean tracer signature, but different Sd values. See lines 346-365.*

16. Line 330: This is not clearly understandable from the table. Consider replacing it with a boxplot.

Reply: Done. See Figs. 3 in the revised manuscript.

17. Line 346: So, do the bars represent the spatio-temporal standard deviation?

Reply: The bars just represent the minimum and maximum values of each tracer signature.

18. Line 356: This sentence is not clear. Please, specify.

Reply: Modified as "Tracer signatures of rainfall are assumed as the same as the tracer signatures of precipitation samples in all the three seasons". See line 227.

19. Line 466: This holds true for this specific study and perhaps for other catchments (not only glaicerized) but not necessarily for all. This should be noted in the discussion.

Reply: Modified as "Sd values are likely overestimated in this study due to small sample sizes, and thus insufficiently representing the variability of the tracer signatures of the corresponding water sources across the basin." See lines 560-561.

20. Line 469: Sampling occasionally not necessarily lead to sharp changes! Please, explain.

Reply: Modified as "Due to the limited accessibility of the sampled sites caused by snow cover, the samples of meltwater and groundwater are often collected sporadically. The small sample size and strong variability in sampled tracers likely lead to a large Sd value." See lines 562-564.

21. Table 1: This table is quite long and dense. Please, consider replacing it with box-plots.

Reply: This table has been split into three sub-tables. Boxplots have been added to present the variability of tracer signatures.

22. Table 4: Perhaps reporting the mean and the SD is clearer than reporting the mean and the range. Please, consider this possible change.

Reply: The ranges of minimum and maximum contributions are used to represent the uncertainty ranges. Sd values have been added in the table. See Table 4.

<u>Reviewer 3:</u>

1. General comments: The study of He and his co-authors presents novel insights into tracer-based hydrograph separation using a comparative approach of evaluating traditional against Bayesian EMMA. In this context, the study aims at filling this important research gap in tracer hydrology both from a methodological and process-oriented point of view. The study shows that the Bayesian approach estimates smaller uncertainties and is less sensitive to sampling uncertainties. The study approach also accounts for isotope fractionation, when using EMMA. Beside only minor comments, I think that the study is mature and presents a concise story line to the readership. The references are with up-to-date and a good use of English can be attributed. After revision of few comments, I can recommend this manuscript for further acceptance in this journal.

Reply: Thanks a lot for the positive comments. We have addressed all your concerns in this revised manuscript.

2. Page 6, Line 153: Please use the PALMEX reference (see below).

Reply: Done. Thanks.

3. Page 6, Line 175: Please clarify if the measurement precision is the same for both LGR and Picarro instruments, otherwise add this details.

Reply: Both measurement precisions of $\delta^{18}O$ and $\delta^{2}H$ are ±0.25 ‰ and ±0.4 ‰, respectively. Specified in the revised manuscript. See line 207.

4. Page 6, Line 178: How did you define 'obvious evaporation'? Did you use a deuterium excess threshold? Please insert further details here. Please add also at which EC limit you discarded samples.

Reply: We used threshold values to identify abnormal values of $\delta^{18}O$ and EC located far away from the sample clusters. For $\delta^{18}O$, sample values higher than 5‰ were excluded. For EC, sample values higher than 210 µs/cm were excluded. We specified that in the revised manuscript. See lines 214-217.

5. Page 6, Line 181: Please correct to 'cold season'; Page 15, Line 438: 'In average'.

Reply: Done. Thanks.

6. Page 8, Line 225: Eqs. 1 -5 hold for 3-components and 2-tracer mixing models. Please provide further information on how you inferred 4 components using 3 tracers.

Reply: When quantifying four runoff components using three tracers, four conservative equations for $\delta^{18}O$, $\delta^{2}H$, EC, and water volume are used (similar to Eq.1). The values of $\delta^{18}O$ and $\delta^{2}H$ are typically correlated for each runoff component. However, the coefficients representing the correlation between $\delta^{18}O$ and $\delta^{2}H$ vary among the runoff components in *glacierized catchment (see Figure 2), thus providing a basis for the EMMA_4 to quantify four runoff components using four conservation equations. The contributions of runoff components (f_i) as well as the partial derivatives used to calculate the uncertainty are solved from the four conservative equations using Matlab. However, the solutions are too lengthy to show in the text. We specified these in the revised manuscript. See lines 267-273.*

7. Page 10, Line 293 – 295: Why did you not analyze the snowmelt uncertainty in the snowmelt period? Besides, the sentence is not clear to me: snowmelt is indeed more difficult to sample in the glacier melt season but easier to sample in the snowmelt period. Also its spatio-temporal variability is much higher in that period of time when most of the melting occurs.

Reply: We investigated the effects of sampling uncertainty only in the glacier melt season because of the following two reasons: (1) Runoff in the glacier melt season contributes the largest part to annual runoff in our study basin. Accurate quantification of each runoff component in this season is extremely important for the understanding of dynamics of water availability in the study area. (2) In this season more meltwater samples are available (15 snowmelt samples and 23 glacier melt samples) than in the snowmelt season (only 15 snowmelt, Table 1), thus providing a good observation data basis for the investigation experiment. Snowmelt sampling in the snowmelt season in the study basin is also difficult due to the heavy snow accumulation in March to April and the spring flood in May to June. However, we believe the effects of snowmelt sampling uncertainty on the end-member mixing approaches in the snowmelt season should be similar to those of meltwater sampling in the glacier melt season. We explained this issue in the revised manuscript. See lines 365-373.

8. Page 11, Line 308: Please provide more information on the fractionation effect and how you represented it in your analysis.

Reply: The water sources for runoff, such as rainfall and meltwater, are subject to evaporation before reaching the basin outlet, especially in summer. However, the isotopic composition of stream water was measured at the basin outlet, and the contributions of runoff components are quantified for the total runoff at the basin outlet. After the long routing path from the sampled sites to the basin outlet, the isotopic compositions of rainfall and meltwater mixing at the basin outlet could be different from those measured at the sampled sites, caused by the evaporation fractionation effect. The isotopic composition of water sources at the sample sites are assumed to be normally distributed in Eqs. 6-7, and the changes in the isotopic compositions of water sources caused by the evaporation fractionation effect are represented by the modification variables $\xi^{18}O$ and $\xi^{2}H$ *in Eq. 10. Parameters describing the prior distributions of isotopic* *compositions at the sample sites in Eqs. 6-7 are estimated by the likelihood observations of isotope signatures of water samples. The modification variables* ξ^{18}O *and* $\xi^{2}H$ *are estimated by the likelihood observations of isotope signatures of stream water. The fractionation effect on the estimated CRC is quantified by comparing two Bayesian scenarios. In the first scenario (using Bayesian_3_OHcor and Bayesain_4_OHcor), the isotopic compositions of water sources at the basin outlet are assumed the same as those measured from the sample sites even though the water sources have suffered evaporation before reaching the basin outlet (using Eqs. 6-9). In the second scenario (using Bayesian_3_OHcor_Frac and Bayesian_4_OHcor_Frac), the evaporation fractionation effect on the isotopic compositions of water sources is considered, and the mixing of water tracers of stream water is represented by Eq.10. We added these explains in the revised manuscript. See lines 375-392. Figure 9 illustrates the effects of fractionation on the quantification of runoff components in all three seasons. The estimated changes in* $\delta^{18}O$ *of each water source are presented in Figs. 9a-c, and the contributions of runoff components quantified by the two scenarios are compared in Figs. 9d-f*

9. Page 11, Line 319: It seems that this sentence contradicts with the one in line 326-328. How can glacier melt have high EC if it has low interaction with mineralized surfaces? Please rephrase both parts accordingly.

Reply: Line 319 has been modified as: "Among the water sources, snowmelt and glacier melt tend to have the lowest EC values." Lines 326-328 have been rephrased as: "The highest CV value of EC for glacier melt indicates large variability in the glacier melt samples. This is because the glacier melt water samples were collected from a rather clean location (EC value is only 1.5 µs/cm) and a relatively dusty location (EC value is 33.4 µs/cm)." See lines 408-409 and 422-425.

10. Page 14, Line 379 –381: This sentence should be moved to the discussion part.

Reply: Modified as: "The EMMA_3 estimated the largest uncertainty ranges and Sd values for CRC in all the three seasons, followed by Bayesian_3_OHind."

11. Page 16, Line 469: Please clarify. How can samples taken occasionally lead to sharp changes of the isotopic composition? Moreover, randomly taken samples may be part of a strategy to represent tracer variability.

Reply: Modified as "Due to the limited accessibility of the sample sites caused by snow cover, the water samples of meltwater and groundwater are often collected sporadically. The small sample size and strong variability in sampled tracers likely lead to a large Sd value." See lines 562-564.

Comparing Bayesian and traditional end-member mixing approaches for hydrograph separation in a glacierized basin

Zhihua He[1,#], Katy Unger-Shayesteh[3], Sergiy Vorogushyn[1], Stephan M. Weise[4], Doris Duethmann[5], Olga Kalashnikova[6], Abror Gafurov[1], Bruno Merz[1,2]

[1]GFZ German Research Centre for Geosciences, Section Hydrology, Telegrafenberg, Potsdam, Germany.

[2]University of Potsdam, Institute for Environmental Sciences and Geography, Potsdam, Germany

[3]Now at German Aerospace Center (DLR), International Relations, Linder Höhe, Cologne, Germany

[4]UFZ Helmholtz Centre for Environmental Research UFZ, Department Catchment Hydrology, Halle Germany

[5]Institute of Hydraulic Engineering and Water Resources Management, Vienna University of Technology (TU Wien), Vienna, Austria

[6]CAIAG Central Asian Institute of Applied Geosciences, Department Climate, Water and Natural Resources, Bishkek, Kyrgyzstan

[#]Now at Centre for Hydrology, University of Saskatchewan, Saskatoon, Saskatchewan, Canada

Manuscript submitted to Hydrology and Earth System Sciences

Abstract

~~Water tracer~~Tracer data have been successfully used for hydrograph separation in glacierized basins. However, uncertainties in the hydrograph separation are large in these basins, caused by the spatio-temporal variability in the tracer signatures of water sources, the uncertainty of water sampling and the mixing model uncertainty. In this study, we used electrical conductivity (EC) measurements and two isotope signatures ($\delta^{18}O$ and $\delta^{2}H$) to label the runoff components, including groundwater, snow and glacier meltwater, and rainfall, in a Central Asia glacierized basin. The contributions of runoff components (CRC) to the total runoff, as well as the corresponding uncertainty, were quantified by two mixing approaches: a traditional end-member mixing approach (~~TEMMA~~abbreviated as EMMA) and a Bayesian end-member mixing approach. The performance of the two mixing approaches ~~were~~was compared in three seasons, distinguished as cold season, snowmelt season and glacier melt season. Results show that: 1) The Bayesian approach generally estimated smaller uncertainty ranges for the CRC compared to the ~~TEMMA~~EMMA. 2) The Bayesian approach tended to be less sensitive to the sampling uncertainties of meltwater than the ~~TEMMA~~EMMA was. 3) Ignoring the model uncertainty caused by the isotope fractionation likely ~~leaded~~led to an overestimated rainfall contribution and an underestimated meltwater share in the melt seasons. Our study provides the first comparison of the two end-member mixing approaches for hydrograph separation in glacierized basins, and gives insights for the application of tracer-based mixing approaches for similar basins.

1. Introduction

Glaciers and snowpack store a large amount of fresh water in glacierized basins, thus providing an important water source for downstream human societies and ecosystems (Barnett et al., 2005; Viviroli et al., 2007; He et al., 2014; Penna et al., 2016). Seasonal meltwater and rainfall play significant roles in shaping the magnitude and timing of runoff in these basins (Rahman et al., 2015; Pohl et al., 2017). Quantifying the seasonal contributions of the runoff components (CRC), including groundwater, snowmelt, glacier melt and rainfall, to the total runoff is therefore highly needed for the understanding of the dynamics of water ~~resource~~resources in glacierized basins under the current climate warming (La Frenierre and Mark, 2014; Penna et al., 2014; He et al., 2015).

The traditional end-member mixing approach (~~TEMMA~~abbreviated as EMMA) has been widely used for hydrograph separation in glacierized basins across the world (Dahlke et al., 2014; Sun et al., 2016a; Pu et al., 2017). For instance, studies in the Italian glacierized Alpine catchments indicate the successful application of the ~~TEMMA~~EMMA to estimate the proportions of groundwater, snow and glacier meltwater based on water stable isotopes and electric conductivity (EC) (e.g., Chiogna et al. 2014, Engel et al. 2016 and Penna et al. 2017). Li et al. (2014) confirmed significant contributions of snow and glacier melt runoff to total runoff in the Qilian Mountains using ~~TEMMA~~EMMA. Maurya et al. (2011) reported the contribution of glacial ice meltwater to the total runoff in a Himalayan basin on $\delta^{18}O$ and EC, using a three-component ~~TEMMA~~EMMA.

However, ~~difficulties in field sampling and seasonal inaccessibility often limit the application of TEMMA in high-elevation glacierized basins (Rahman et al., 2015). Moreover,~~ uncertainties ~~for the~~in CRC quantified by ~~the TEMMA~~ EMMA in glacierized basins are typically high (Klaus and McDonnell, 2013; Rahman et al., 2015)~~, which can be caused by,~~ because of the following reasons: (1) The catchment elevation generally extends over a large range, leading to strong spatial variability in climate forcing (precipitation and temperature) and the tracer signatures of water sources; (2) The number of end-member water sources for runoff is typically high, additionally including snow and glacier meltwater; (3) Water sampling in high-elevation glacierized catchment is difficult due to the logistical limitations, resulting in small sample sizes for the application of EMMA. Uncertainties in CRC quantified by the EMMA can be categorized into statistical uncertainty and model uncertainty. Statistical uncertainty refers to the spatio-temporal variability ~~for~~of the tracer signatures, sampling uncertainty and laboratory measurement error (Joerin et al., 2002). Model uncertainty is determined by the assumptions of the ~~TEMMA~~EMMA, which might not agree with reality

(Joerin et al., 2002; Klaus and McDonnell, 2013). For example, the fractionation effect on isotope ratios caused by evaporation during the mixing process can result in significant errors given the constant tracer assumption in the ~~TEMMA~~EMMA (Moore and Semmens, 2008).

The Gaussian error propagation technique has been typically applied along with ~~TEMMA~~EMMA to estimate the statistical uncertainty for ~~the~~ hydrograph separation, assuming the uncertainty associated with each source is independent from the uncertainty of other sources (Genereux, 1998; Pu et al., 2013). The spatio-temporal variability ~~for~~of the tracer signatures is estimated by multiplying the *t* values of the Student's *t* distribution at the selected significance level with the standard deviations (*Sd*) of the measured tracer signatures (Pu et al., 2013; Penna et al., 2016; Sun et al., 2016b). Although this approach has been successfully used in various glacierized basins, some recurring issues remain. These include (1) inappropriate estimation of the variability of tracer signatures of water sources when only few water samples are available (Dahlke et al., 2014)~~, and (2) negligence~~. The used *Sd* values of the measured tracer signatures likely fail to represent the variability of tracer signatures of individual water sources across the basin, due to the small water sample sizes; (2) The correlation of ~~water tracers~~tracer signatures and runoff components ~~caused by the~~ are inevitably ignored, due to the assumption of independence of the multiple uncertainty sources. The correlation between $\delta^{18}O$ and $\delta^{2}H$ of each water source, as well as the interaction between runoff components could provide additional constraints on the uncertainty in the quantification of runoff components, which however are typically ignored in the Gaussian error propagation technique. Further, the model uncertainty caused by the fractionation effect on isotope ratios during the mixing process is also often ignored.

The Bayesian end-member mixing approach (abbreviated as Bayesian approach) shows the potential to estimate the proportions of individual components to the mixing variable in a more rigorous statistical way (Parnell et al., 2010). For hydrograph separation, the ~~water~~ tracer signatures of the water sources are first assumed to obey specific prior distributions. Their posterior distribution are then obtained by updating the prior distributions with the ~~observation~~ likelihood observations derived from water samples. In the last step, ~~the~~ CRC to the total runoff are estimated based on the balance of the posterior ~~water~~ tracer signatures. The posterior distributions~~, expressing the uncertainties for~~ of the CRC ~~and parameters,~~ are typically estimated in a Markov Chain Monte Carlo (MCMC) procedure. In the Bayesian approach, both the statistical and model uncertainties are represented by the posterior distributions of parameters. The parameter uncertainty is estimated based on likelihood observations using MCMC.

Although the Bayesian approach can be applied in~~-~~ cases when the sample sizes are small (Ward et al., 2010), it has been rarely used for hydrograph separation in glacierized basins. To the authors' knowledge, there have been only three studies, including Brown et al. (2006), who conducted the hydrograph separation in a glacierized basin in the French Pyrenees using a three-component Bayesian approach. Further, Cable et al. (2011) quantified the CRC to total runoff in a glacierized basin in the American Rocky Mountains. They used a hierarchical Bayesian framework to incorporate temporal and spatial variability in the water isotope data into the mixing model. Recently, Beria et al. (2019) used a classic Bayesian approach to estimate the uncertainty ~~for the~~in CRC in a Swiss alpine catchment. However, the performance of the Bayesian approach has not been ~~compared~~evaluated in comparison to the ~~TEMMA~~EMMA. Moreover, the sensitivity of the Bayesian approach to the water sampling uncertainty associated with the representativeness of the water samples caused by the limited sample site and sample size is still not clear. ~~The potential of the~~ Benefiting from the prior assumptions for changes in isotope signatures during the mixing process, the Bayesian approach bears the potential to estimate the fractionation effect on isotopic signatures ~~during the mixing process~~(Moore and Semmens, 2008), which however, has not been investigated either.

In this study, we compare ~~TEMMA~~EMMA and the Bayesian approach for hydrograph separation in a Central Asia glacierized basin, using water isotope and EC measurements. ~~The~~In Central Asia, glacierized catchments provide important fresh water supply for downstream cities and irrigated agriculture. Quantifying the contributions of multiple runoff components to total runoff is important for understanding the dynamics of water resource availability at the regional scale. However, uncertainty in the quantification of runoff components in the glacierized catchments are particularly large as mentioned before. Our research questions are two-fold: 1) How do ~~TEMMA~~EMMA and~~ the~~ Bayesian approaches compare with respect to the quantification ~~for the~~of CRC? 2) What is the influence of the different uncertainty sources (including variability of the tracer signatures, sampling uncertainty, and model uncertainty) on the estimated CRC in the two mixing approaches?

The paper is organized as follows: ~~details~~Details on the study basin and water sampling are introduced in Section 2; ~~assumptions~~Assumptions of the two mixing approaches are described in Section 3; Section 4 estimates the CRC, as well as the corresponding uncertainties; ~~discussion~~Discussion and conclusion finalize the paper in Sections 5 and 6, respectively.

2. Study area and data

2.1 Study area

Located in Kyrgyzstan, Central Asia, the Ala-Archa basin drains an area of 233 km^2, (Fig. ~~1), and glacier covers around 17% of the basin area. The elevation of the study basin extends from 1560 m to 4864 m a.s.l..~~1), and glaciers cover around 17% of the basin area. The elevation of the study basin extends from 1560 m to 4864 m a.s.l., and the elevation range of the glacierized area extends from 3218 to 4857 m a.s.l., with about 76% located between 3700 and 4100m a.s.l.. The Golubin glacier has an area of ~5.7 km^2 and extends over an elevation range from 3232 to 4458 m a.s.l. (Fig. 1). Both the elevation range and the mean elevation (3869 m a.s.l.) of the Golubin glacier are close to those of the entire glacierized area (mean elevation is 3945 m a.s.l.). The Golubin glacier represents about 14.4% of the entire glacierized area, while its elevation range covers around 95.6% of the entire glacier range. The annual mean precipitation and air temperature measured at the Baitik meteorological station during 2012-2017 are 538 mm yr^{-1} and 7.2 ℃, respectively. The mean daily streamflow during 2012-2017 is about 6.3 m^3/s (Fig. S1). The seasonal dynamics of runoff in the river play an important role in the water availability for downstream agricultural irrigation. The generation of snow and glacier melt runoff generally ~~show~~shows the largest effect on the runoff seasonality (Aizen et al., 2000; Aizen et al., 2007). In particular, the snowmelt runoff mainly occurs in the warm period from early March to middle September, and the glacier melt typically generates runoff from the high-elevation areas during July to September (Aizen et al., 1996; He et al., 2018; He et al., 2019). We subsequently defined three runoff generation seasons as follows. Cold season: from October to February, in which the streamflow is fed mainly by groundwater and to a smaller extent by snowmelt and rainfall; Snowmelt season: from March to June, in which the streamflow is fed chiefly by snowmelt and groundwater and additionally by rainfall; Glacier melt season: from July to September, in which the streamflow is fed by significant glacier melt and groundwater, rainfall and snowmelt.

Two meteorological stations (Fig. 1), i.e., Alplager (at elevation of 2100 m a.s.l.) and Baitik (at elevation of 1580 m a.s.l.), have been set up in the basin since the 1960s to collect daily precipitation and temperature data. The Ala-Archa hydrological station has been set up at the same site of the Baitik meteorological station to collect daily average ~~discharge~~streamflow data since the 1960s. The dynamics of glacier mass balance and snow mass balance in the accumulation zone have been surveyed in summer field campaigns through 2012-2017. Daily precipitation, temperature and streamflow measured at the basin outlet during 2012-2017, are presented in Fig. S1 in the supplement file.

2.2 ~~Water tracer~~Tracers data

Formatted: Font: Italic

Since July of 2013, stream water samples have been collected weekly by local station operators, from the river channel close to the Alplager and Baitik meteorological sites, using pure ~~plastic~~50 ml high-density polyethylene (HDPE) bottles (He et al., 2019). The sampling time slightly varied around noon every Wednesday. Precipitation samples were collected during 2012-2017 at four sites across the basin (Fig. 1). At the Alplager and Baitik meteorological sites, the precipitation samples were first collected from fixed rain collectors (immediately after the rainfall/snowfall events), and then accumulated in two indoor rain containers over one month. The mixed water in the containers were then sampled for isotopic analysis every month. The indoor rain containers were filled with thin mineral oil layers for monthly precipitation accumulation and stored in cold places. Additionally, two plastic rain collectors PALMEX~~,~~ (similar to Gröning et al., 2012), specifically designed for isotopic sampling to prevent evaporation, were set up at~~ the~~ elevations of 2580 m a.s.l. and 3300 m a.s.l. to collect precipitation in high-elevation areas (Fig. 1). Precipitation samples were collected monthly from these two rain collectors during the period from May to October when the high-elevation areas were accessible.

Glacier meltwater ~~were~~was sampled during the summer field campaigns in each year of 2012-2017. Samples of meltwater flowing on the Golubin glacier in the ablation zone and at the glacier tongue were collected by pure ~~plastic~~50 ml HDPE bottles and then stored in a cooling box (Fig. 1, the elevation of the sampling sites ranges from 3280 m to 3805 m a.s.l.). We only collected glacier meltwater samples from the Golubin glacier due to the logistic limitations in the remaining glacierized area. Snow samples were collected ~~through~~from early March to early October during 2012-2017, as the sampling sites are generally not accessible ~~caused by~~due to the heavy snow accumulation in the remaining months. The elevation of the multiple snow sampling sites ranges from 1580 m to 4050 m a.s.l. (Fig. 1). The whole snow profile at each sampling site was collected through drilling a 1.2 m pure plastic tube into the snowpack. The snow in the whole tube were then collected by plastic bags and stored in a cooling box. After all the snow in the plastic bags melted out, the mixed snow meltwater samples were then ~~sampled~~collected by pure ~~plastic~~HDPE bottles. Groundwater samples were also collected through March to October during 2012-2017, from a spring draining to the river (Fig. 1, 2400 m a.s.l.) using pure ~~plastic~~HDPE bottles. The spring is located at the foot of a rocky hill, around 60 meters away from the river channel.

All samples were stored at 4 ℃ and then delivered to the laboratory ~~of~~at Helmholtz Center for Environmental Research (UFZ) in Halle of Germany by flight. Isotopic compositions of water samples were measured using a Laser-based infrared spectrometry (LGR TIWA 45, Picarro L1102-i). A regular calibration has been carried out to minimize the memory effect. The measurement precisions of both LGR TIWA 45 and Picarro L1102-i for $\delta^{18}O$ and $\delta^{2}H$ are~~:~~ ±0.25 ‰ and ±0.4 ‰, respectively, after the calibration against the common VSMOW standard. We used the Hanan Instruments HI-9813 PH EC/TDS portable meter to measure the EC values of ~~the~~ water samples~~ were measured using portable PH/TDS/EC meters.~~, with a measurement precision of 0.1 µs/cm. EC data has been widely used for hydrograph separation, due to its easy use and quick measurement. While EC is not a conservative tracer, this may have only small effects on the application of hydrograph separation at the catchment scale. Abnormal isotopic compositions caused by ~~obvious~~ evaporation and abnormal EC values caused by impurities were discarded. We used threshold values to identify abnormal values of $\delta^{18}O$ and EC located far away from the sample clusters. For $\delta^{18}O$, sample values higher than 5‰ were excluded. For EC, sample values higher than 210 µs/cm were excluded. Tracers data of individual water sources at the sampled date are presented in Fig. S1.

3. Methodology

The hydrograph separation is carried out in each of the three seasons (i.e., ~~clod~~cold season, snowmelt season and glacier melt season). Water samples collected in the period from 2012 to 2017 are ~~distributed~~split into each of the three seasons for the hydrograph separation. The CRC estimated by the mixing approaches refer to the mean contributions in each of the three seasons during the period of 2012-2017~~, i.e., the inter-annual variability of CRC were not considered.~~. The mixing approaches applied for the hydrograph separation in each season are summarized in Table 2. Considering the groundwater and snowmelt samples were rarely collected in the cold season, we used all available groundwater and snowmelt samples from the three seasons for hydrograph separation in the cold season. Tracer signatures of rainfall are assumed as same as the measured tracer signatures of precipitation samples in all the three seasons.

3.1 Traditional end-member mixing approach (~~TEMMA~~EMMA)

The main assumptions of ~~TEMMA~~EMMA are as follows (Kong and Pang, 2012): (1) The ~~water~~ tracer signature of each runoff component is constant during the analyzed period; (2) The ~~water~~ tracer signatures of the runoff components are significantly different from each other; (3) ~~Water tracer~~Tracer signatures are conservative in the mixing process. In the cold and snowmelt seasons, a three-component ~~TEMMA~~EMMA method (~~TEMMA~~EMMA_3, Table 2) is used. Since the precision of $\delta^{18}O$ (±0.25 ‰) measured in the lab is higher than that of $\delta^{2}H$ (±0.4 ‰) and both are strongly correlated, the ~~TEMMA~~EMMA_3 is based on $\delta^{18}O$ and EC. In the glacier melt season, both the ~~TEMMA~~EMMA_3 and the four-component ~~TEMMA~~

Formatted: Font: Italic

Formatted: Font: Italic

Formatted: German (Germany)

~~(TEMMA~~EMMA (EMMA_4, Table 2) are used. In the ~~TEMMA~~EMMA_3, glacier melt and snowmelt are assumed as one end-member, considering their similar tracer signatures. In the ~~TEMMA~~EMMA_4, glacier melt and snowmelt are treated as two end-members separately, and $\delta^{18}O$ and $\delta^{2}H$ are used as two separate tracers. The following equations (Eqs. 1-5) are used to estimate CRC ($f_{1\text{-}3}$) and the corresponding uncertainty in the ~~TEMMA~~EMMA_3 (Genereux, 1998).

$$\begin{cases} 1 = f_1 + f_2 + f_3, & \textit{for water balance} \\ A = A_1 \cdot f_1 + A_2 \cdot f_2 + A_3 \cdot f_3, & \textit{for water tracer } A \\ B = B_1 \cdot f_1 + B_2 \cdot f_2 + B_3 \cdot f_3, & \textit{for water tracer } B \end{cases} \tag{1}$$

$$f_1 = \frac{AB_2 - AB_3 + A_2B_3 - A_2B + A_3B - A_3B_2}{A_1B_2 - A_1B_3 + A_2B_3 - A_2B_1 + A_3B_1 - A_3B_2} \tag{2}$$

$$f_2 = \frac{AB_3 - AB_1 + A_1B - A_1B_3 + A_3B_1 - A_3B}{A_1B_2 - A_1B_3 + A_2B_3 - A_2B_1 + A_3B_1 - A_3B_2} \tag{3}$$

$$f_3 = \frac{AB_1 - AB_2 + A_1B_2 - A_1B + A_2B - A_2B_1}{A_1B_2 - A_1B_3 + A_2B_3 - A_2B_1 + A_3B_1 - A_3B_2} \tag{4}$$

where the subscripts 1-3 refer to the three runoff components (i.e., groundwater, snowmelt/meltwater and rainfall), and A_1-A_3 (B_1-B_3) refers to the mean $\delta^{18}O$ (EC) values of runoff components. A and B stand for the mean $\delta^{18}O$~~-~~ and EC values of the stream water. The mean isotope and EC values of precipitation are calculated as the monthly precipitation weighted average values. Similarly, the mean isotope and EC values of stream water are calculated as the weekly streamflow weighted average values.

Assuming the uncertainty of each variable is independent from the uncertainty in others, the Gaussian error propagation technique is applied to estimate the uncertainty of the CRC ($f_{1\text{-}3}$) using the following equation (Genereux, 1998):

$$W_{f_i} = \sqrt{(\frac{\partial f_i}{\partial A_1}W_{A_1})^2 + (\frac{\partial f_i}{\partial A_2}W_{A_2})^2 + (\frac{\partial f_i}{\partial A_3}W_{A_3})^2 + (\frac{\partial f_i}{\partial A}W_{A})^2 + (\frac{\partial f_i}{\partial B_1}W_{B_1})^2 + (\frac{\partial f_i}{\partial B_2}W_{B_2})^2 + (\frac{\partial f_i}{\partial B_3}W_{B_3})^2 + (\frac{\partial f_i}{\partial B}W_{B})^2} \tag{5}$$

where f_i stands for the contribution of a specific runoff component, and W is the uncertainty in the variable specified by the subscript. For the uncertainty of ~~water~~ tracer signatures (W_{A_i} and W_{B_i}), we multiply the *Sd* values of the measured tracer signatures with *t* values from the Student's *t* value table at the confidence level of 95%. The degree of freedom for the Student's *t* distribution is estimated as the number of water sample for each water source minus one. Analytical measurement errors are not considered in this approach, which, however, are minor compared to the uncertainty generated from ~~water~~ tracer variations (Penna et al., 2017; Pu et al., 2017). The *lsqnonneg* function in Matlab is used to solve Eqs.

1-4, which solves the equations in a least squares sense, given the constraint that the solution vector $\boldsymbol{f}$ has nonnegative elements. ~~The TEMMA_4 uses the equations similar to Eqs. 1-5~~The EMMA_4 uses the equations similar to Eqs. 1-5. The values of $\delta^{18}O$ and $\delta^{2}H$ are typically correlated for each water source. However, the coefficients representing the correlation between $\delta^{18}O$ and $\delta^{2}H$ vary among the water sources in glacierized catchment, thus providing a basis for the EMMA_4 to quantify four runoff components. When quantifying four runoff components using three tracers, four conservative equations for $\delta^{18}O$, $\delta^{2}H$, EC, and water volume are used (similar to Eq.1). The contributions of runoff components ($\boldsymbol{f}$), as well as the partial derivatives used to calculate the uncertainty are solved from the four conservative equations using Matlab. However, the solutions are too lengthy to show in the text.

3.2 Bayesian mixing approach

The Bayesian approaches applied for each season are summarized in Table 2. Similar to the ~~TEMMA~~EMMA, we apply a three-component Bayesian approach to all seasons, and additionally a four-component Bayesian approach in the glacier melt season. The three-component Bayesian approach has two types: the Bayesian_3_~~Cor~~OHcor approach considers the correlation between $\delta^{18}O$ and $\delta^{2}H$, whereas the Bayesian_3_OHind approach assumes independence. The four-component Bayesian approach also has two types: Bayesian_4_~~Cor~~OHcor considering the correlation, and Bayesian_4_OHind assuming independence between $\delta^{18}O$ and $\delta^{2}H$. ~~The~~A Kolmogorov-Smirnov test has been carried out for both isotope and EC tracers of all water sources before the applicaiton of Bayesian approaches. The tracer data of runoff components (i.e., rainfall, snowmelt, groundwater and glacier melt) generally pass the normal distribution test at significance levels of p-values > 0.3, while the tracer data of stream water fail to pass the normal distributions test partly caused by the extreme isotope and EC values (see Figs. S1a-b). The EC data of glacier melt also fail to pass the normal distribution test, which can be caused by the low sample size. Thus, the prior assumptions for the Bayesian approaches are listed as follows (similarly to Cable et al. 2011): In approaches considering the correlation between $\delta^{18}O$ and $\delta^{2}H$, the prior distributions of $\delta^{18}O$ and $\delta^{2}H$ of runoff components ~~and stream water~~ are assumed as bivariate normal distributions with means and precision matrix as $\mu^{18}O$, $\mu^{2}H$ and $\boldsymbol{\Omega}$, respectively (Eq.6a). The precision matrix ($\boldsymbol{\Omega}$, i.e. the inverse of the covariance matrix) for the two isotopes is assumed as Wishart prior (Eq. 6b). When assuming independence between $\delta^{18}O$ and $\delta^{2}H$, the prior distributions of $\delta^{18}O$ ($\delta^{2}H$) of runoff components ~~and stream water~~ are assumed as normal distributions with means and variance of $\mu^{18}O$ and $\lambda^{18}O$ ($\mu^{2}H$ and $\lambda^{2}H$, Eqs. 6c-d). The mean values of the isotopes of runoff components (i.e., μ^{18}O and μ^{2}H) are further estimated by independent normal priors (Eq. 7, Cable et al. 2011), which is assumed to consider the spatial variability of μ^{18}O and μ^{2}H.

$$\begin{cases} \begin{bmatrix} \delta^{18}O \\ \delta^{2}H \end{bmatrix} \sim Multi\_normal\left(\begin{bmatrix} \mu^{18}O \\ \mu^{2}H \end{bmatrix}, \Omega\right) & (6a) \\ \boldsymbol{\Omega} \sim Wishart\ (2, \boldsymbol{V}) & (6b) \\ \delta^{18}O \sim Normal\ (\mu^{18}O, \lambda^{18}O) & (6c) \\ \delta^{2}H \sim Normal\ (\mu^{2}H, \lambda^{2}H) & (6d) \end{cases}$$

$$\begin{cases} \mu^{18}O \sim Normal\ (\gamma^{18}O, \sigma^{18}O) & (7a) \\ \mu^{2}H \sim Normal\ (\gamma^{2}H, \sigma^{2}H) & (7b) \end{cases}$$

where, λ^{18}O, γ^{18}O and σ^{18}O (λ^{2}H, γ^{2}H and σ^{2}H) are parameters used to describe the normal priors of δ^{18}O and μ^{18}O (δ^{2}H and μ^{2}H, see Table 3), which are estimated by likelihood observations ~~(Table 3).~~. $\boldsymbol{V}$ is a 2*2 unit positive-definite matrix, and '2' stands for the degree of freedom in the Wishart prior distribution.

The priors of EC values of runoff components ~~and stream water~~ are assumed as normal distributions (Eq. 8a), with mean ε and variance τ. Similarly, the spatial variability of the mean EC values of runoff components (ε) are assumed to follow a normal distribution with mean θ and variance ω (Eq. 8b). τ, θ and ω are parameters estimated by likelihood observations (Table 3).

$$\begin{cases} EC \sim Normal\ (\varepsilon, \tau) & (8a) \\ \varepsilon \sim Normal\ (\theta, \omega) & (8b) \end{cases}$$

The prior distributions of stream water are calculated in two steps. First, the prior distributions of δ^{18}O, δ^{2}H and EC of stream water are assumed as same as those of runoff components in Eqs. 6 and 8a. Second, the

$$\begin{cases} \begin{bmatrix} \mu^{18}O \\ \mu^{2}H \\ \varepsilon \end{bmatrix}_{stream\ water} = \sum_{i=1}^{N} f_i \cdot \begin{bmatrix} \mu^{18}O \\ \mu^{2}H \\ \varepsilon \end{bmatrix}_{runoff\ component\ i} & (9a) \\ \boldsymbol{f} \sim Dirichlet(\boldsymbol{\alpha}) & (9b) \\ \boldsymbol{\alpha} = \boldsymbol{\rho} + \boldsymbol{\psi} & (9c) \\ [\boldsymbol{\rho}, \boldsymbol{\psi}] \sim Multi\_normal(\boldsymbol{\beta}, \boldsymbol{\Omega}) & (9d) \end{cases}$$

~~The~~ mean isotopes (μ^{18}O and μ^{2}H) and EC (ε) of stream water are constrained by a mixing model (Eqs. 9a-b), which estimates the isotope and EC mean values of stream water by multiplying the contribution of each runoff component (f_i) with the corresponding mean isotope and EC values of each runoff component (Eq. 9a).

$$\begin{cases} \begin{bmatrix} \mu^{18}O \\ \mu^{2}H \\ \varepsilon \end{bmatrix}_{stream\ water} = \sum_{i=1}^{N} f_i \cdot \begin{bmatrix} \mu^{18}O \\ \mu^{2}H \\ \varepsilon \end{bmatrix}_{runoff\ component\ i} & (9a) \\ \boldsymbol{f} \sim Dirichlet(\boldsymbol{\alpha}) & (9b) \\ \boldsymbol{\alpha} = \boldsymbol{\rho} + \boldsymbol{\psi} & (9c) \\ [\boldsymbol{\rho}, \boldsymbol{\psi}] \sim Multi\_normal(\boldsymbol{\beta}, \boldsymbol{\Omega}) & (9d) \end{cases}$$

~~In this equation~~where, N is the number of runoff components. The contribution vector ($\boldsymbol{f}$) is represented by a Dirichlet distribution with an index vector $\boldsymbol{\alpha}$ (Eq. 9b), in which the sum of contributions of all runoff components ($\sum f_i$) equals one. The index vector $\boldsymbol{\alpha}$ is estimated by two variable vectors $\boldsymbol{\rho}$ and $\boldsymbol{\psi}$ (Eq.9c), considering the temporal and spatial variability in the CRC (Cable et al. 2011). $\boldsymbol{\rho}$ and $\boldsymbol{\psi}$ are assumed as bivariate normal distribution with means and precision matrix $\boldsymbol{\beta}$ and $\boldsymbol{\Omega}$ (Eq.9d). $\boldsymbol{\beta}$ is a parameter vector estimated by likelihood observations (Table 3).

Formatted: Indent: First line: 0"

The value ranges for the parameters need to be estimated in Eqs. 6-9 are summarized in Table 3. The posteriors of parameters describing the spatial variability of ~~water tracers~~tracer signatures in Eqs. 7 and 8b are first estimated by the mean ~~water~~ tracer signatures of runoff components measured at different spatial locations. Parameters describing the overall variability of ~~water~~ tracer signatures in Eqs. 6 and 8a are then constrained by the likelihood observations of ~~water~~ tracer signatures from all water samples at different times and locations. The posterior distribution of CRC ($\boldsymbol{f}$) are estimated by Eq. 9, based on the posterior ~~water~~ tracer signatures of runoff components and the measured ~~water~~ tracer signatures from stream water samples. The posteriors of parameters and contributions are estimated by the *R* software package *Rstan*. We run four parallel Markov Chain Monte Carlo (MCMC) chains with 2000 iterations for each chain. The first 1000 iterations are discarded for warm-up, generating a total of 4*1000 samples for the calculation of the posterior distributions. Uncertainties are presented as the 5-95 percentile ranges from the iterative runs. The parameter values are assumed to follow uniform prior distributions within the value ranges to ~~run~~initialize the MCMC procedure.

To be noted, the four-components approaches (EMMA_4, Bayesian_4_OHcor and Bayesian_4_OHind) are developed in our study to investigate the two following questions: (1) Is the EMMA able to quantify four runoff components just using $\delta^{18}O$, $\delta^{2}H$, and EC? (2) Does the correlation between $\delta^{18}O$ and $\delta^{2}H$ help to reduce the uncertainty in the quantification of runoff components? The correlation between $\delta^{18}O$ and $\delta^{2}H$ is ignored in Bayesian_4_OHind. We used independent prior distributions for $\delta^{18}O$ and $\delta^{2}H$ of each water source. In Bayesian_4_OHcor, the posterior parameters describing the correlation between $\delta^{18}O$ and $\delta^{2}H$

vary among the water sources, thus providing a basis for the quantification of four runoff components using four mixing equations of tracer signatures (similar to Eq.9).

3.3 Effects of the uncertainty in the meltwater sampling

Due to limited accessibility, meltwater samples are typically difficult to collect in high-elevation glacierized areas. Often, only small sample sizes are available to represent the tracer signatures of meltwater generated from the entire glacierized area. Hence, the representativeness of meltwater samples ~~can have significant effects on~~implies an additional uncertainty source in the hydrograph separation~~.~~

~~To~~We thus define three virtual sampling scenarios to evaluate ~~this~~the effect ~~for~~of meltwater sampling on the ~~TEMMA~~EMMA and Bayesian mixing approaches~~, we define three virtual sampling scenarios.~~. Scenario I~~:~~ is used to evaluate the effects of sample size of meltwater, in which four groups of meltwater sample are tested. The ~~meltwater~~four sample groups have ~~different sample sizes, but~~ the same mean value and *Sd* of ~~the investigated tracer;~~$\delta^{18}O$ or EC, but different sample sizes. Mean and *Sd* values of $\delta^{18}O$ or EC are calculated for all used meltwater samples in each group, referring to the spatial-temporal variability (same in the two following scenarios). Scenario II~~:~~ is used to evaluate the effects of sampled mean value of $\delta^{18}O$ (or EC) of meltwater. The ~~meltwater~~four sample groups have the same sample size and *Sd*, but different mean values of ~~the investigated tracer, but the same sample size and *Sd* of the investigated tracer;~~$\delta^{18}O$ (or EC). Scenario III~~:~~ is used to investigate the effects of *Sd* values of sampled $\delta^{18}O$ (or EC). The ~~meltwater~~four sample groups have the same sample size and mean tracer signature, but different *Sd* ~~of the investigated tracer, but keeping the same sample size and mean value of the investigated tracer. We only~~values. We investigated the effects of the meltwater sampling uncertainty on the mixing approaches in the glacier melt season, since meltwater is particularly difficult to collect and is the dominant runoff component in this season. For the water samples of other runoff components and stream water, we used all the available measurements in the glacier melt season for the three virtual scenarios, keeping the same sample characteristics. We investigated the effects of sampling uncertainty only in the glacier melt seasons because of the following reasons: (1) Runoff in the glacier melt season contributes the largest part to annual runoff in our study basin. Accurate quantification of each runoff component in this season is extremely important for the understanding of dynamics of water availability in the study area. Quantifying the uncertainty in the contributions of runoff components caused by sampling uncertainty of meltwater is highly needed in this season; (2) There are more meltwater samples available in this season (15 snowmelt samples and 23 glacier melt samples) than in the snowmelt season (only 15 snowmelt, Table 1), thus providing a good observation data basis for the investigation.

3.4 Effects of water isotope fractionation on hydrograph separation

~~To consider the changes on the isotope signatures of runoff components~~The water sources for runoff, such as rainfall and meltwater, are subject to evaporation before reaching the basin outlet, especially in summer. However, the isotopic composition of stream water was measured at the basin outlet, and the contributions of runoff components are quantified for the total runoff at the basin outlet. After the long routing path from the sampled sites to the basin outlet, the isotopic compositions of rainfall and meltwater mixing at the basin outlet could be different from those measured at the sampled sites, caused by the evaporation fractionation effect. To consider the changes in the isotope signatures of water sources caused by the fractionation effect during the mixing process, we set up two modified Bayesian approaches~~, ~~, i.e~~.~~., Bayesian_3_~~Cor_F~~OHcor_Frac and Bayesian_4_~~Cor_F~~OHcor_Frac (Table 2). The ~~effects of water isotope~~ fractionation effect on the ~~hydrograph separation are investigated in virtual experiments~~ estimated CRC is quantified by comparing two Bayesian scenarios. In the first scenario (using ~~the modified approaches.~~Bayesian_3_OHcor and Bayesain_4_OHcor), the isotopic compositions of water sources at the basin outlet are assumed the same as those measured from the sample sites even though the water sources have suffered evaporation before reaching the basin outlet (using Eqs. 6-9). In the second scenario (using Bayesian_3_OHcor_Frac and Bayesian_4_OHcor_Frac), the evaporation fractionation effect on the isotopic compositions of water sources is considered, and the mixing of water tracers for stream water is represented by Eq.10. We modify the mean values in Eq. 9a using fractionation factors ξ^{18}O and ξ^{2}H ~~(Eq. 10)~~. The priors for ξ^{18}O and ξ^{2}H are assumed as bivariate normal distributions in Eq.11.

$$\begin{bmatrix}\mu^{18}O\\ \mu^{2}H\end{bmatrix}_{stream\ water} = \sum_{i=1}^{N} f_i \bullet \begin{bmatrix}\mu^{18}O+\xi^{18}O\\ \mu^{2}H+\xi^{2}H\end{bmatrix}_{runoff\ \ component\ i} \qquad (10)$$

$$\begin{bmatrix}\xi^{18}O\\ \xi^{2}H\end{bmatrix} \sim Multi\_normal\ (\begin{bmatrix}\eta^{18}O\\ \eta^{2}H\end{bmatrix}, \boldsymbol{\Omega}) \qquad (11)$$

where, η^{18}O and η^{2}H are parameters describing the mean values of the changes in isotopes caused by the fractionation effect~~, which are parameters need to be estimated. ~~. $\boldsymbol{\Omega}$ is the inverse of the covariance matrix defined in Eq. 6b. The parameters in Eqs. 6-11 are then re-estimated by the measurements of ~~water tracer signatures using the MCMC procedure.~~tracer signatures using the MCMC procedure. In particular, parameters describing the prior distributions of isotopic compositions at the sample sites in Eqs. 6-7 are estimated by the likelihood observations of isotope signatures of runoff components. The fractionation factors ξ^{18}O and ξ^{2}H are estimated by the likelihood observations of isotope signatures of stream water.

4. Results

4.1 Seasonality of ~~water~~ tracer signatures

Tracer measurements from all the water samples are summarized in Table 1 and Fig. 2~~.~~ (see also Fig. S1). The mean values in Table 1 indicate that precipitation is most depleted in heavy water isotopes (^{18}O and ^{2}H) in the cold season among the water sources. In the melt seasons, snow and glacier meltwater show the most depleted heavy isotopes. The EC values are highest in groundwater in all seasons, followed by stream water and precipitation. Among the water sources, snowmelt and glacier melt tend to have the lowest EC values. Figure 2 shows that the slope of the local meteoric water line (LMWL) is lower than that of the global meteoric water line (GMWL). The δ^{18}O of precipitation and snowmelt range from -22.82‰ to 1.51‰ and from -17.31‰ to -6.95‰, respectively. The isotopic composition of glacier meltwater is more depleted than those of groundwater and stream water. Stream water shows a similar isotopic composition to groundwater. Three samples from the stream water are far below the LMWL, which is ~~Snowmelt and glacier melt tend to have the lowest EC values, due to low interaction with mineral surface.~~ likely caused by the evaporation effect.

CV values in Table 1 and boxplots in Figs. 3a-f show that the δ^{18}O and δ^{2}H of precipitation generally shows the largest variability in all seasons, followed by the isotopes of snowmelt. Groundwater and stream water show the smallest CV values for δ^{18}O in all three seasons. The stream water presents the lowest CV value for EC in all seasons, followed by the groundwater. The snowmelt EC shows high CV values in the snowmelt and glacier melt seasons, which may be attributed to variable dust conditions at the sampling locations (from downstream gauge station to upper glacier accumulation zone). The highest CV value of EC ~~was observed~~ for glacier melt~~, since~~ indicates large variability in the glacier melt samples (see also Figs. 3g-i). This is because the glacier melt water samples were collected ~~at locations with different sediments conditions in the ice (~~from ~~extremely~~a rather clean ~~to heavily~~location (EC value is only 1.5 µs/cm) and a relatively dusty location (EC value is 33.4 µs/cm).

For each water source except groundwater, the ~~water~~ tracer signatures show a significant seasonality (Table 1 and Fig. 3). In particular, the δ^{18}O and δ^{2}H of precipitation are most depleted in the cold season and reach the highest values in the glacier melt season, partly caused by the seasonality in temperature. Stream water shows higher values of δ^{18}O and EC in the cold season when groundwater dominates the streamflow, and has lower values in the melt seasons when meltwater has a dominant contribution. Snowmelt has a lower EC value in the glacier melt season than in the cold and snowmelt seasons. ~~This can be explained by~~ In the ~~fact that the~~ cold and snowmelt seasons, some snowmelt samples also have EC values as low as those in the glacier melt season. The snow samples in the glacier melt season were only collected from the accumulation zone of the glacier, thus resulting in small variability in the EC values. The snowpack in the accumulation zone is accumulated by fresh snow in the snowy period (summer type accumulation ~~area.~~glacier).This leads to low EC values in the snowmelt samples. The ~~water~~ tracer signature of groundwater is relatively stable across the seasons.

Figures 3j-l~~Figure 2 shows that the slope of the local meteoric water line (LMWL) is lower than that of the global meteoric water line (GMWL). The $\delta^{18}O$ of precipitation and snowmelt range from -22.82‰ to 1.51‰ and from -17.31‰ to -6.95‰, respectively. The isotopic composition of glacier meltwater is more depleted than those of groundwater and stream water. Stream water shows a similar isotopic composition to groundwater. Three samples from the stream water are far below the LMWL, which is assumed to be caused by the evaporation effect.~~

~~Figure 3~~ shows the $\delta^{18}O$-EC mixing space of runoff components in the three seasons. The ~~uncertainty bars~~ranges of solid lines indicate the minimum and maximum tracer values ~~represent the temporal and spatial variability~~of individual water samples. In the cold season, the $\delta^{18}O$ and EC values of stream water are very close to those of groundwater (Fig. ~~3a~~3j), whereas the snowmelt and precipitation tracer signatures ~~are different~~show much difference. These results indicate the dominance of groundwater on streamflow during the cold season. In the snowmelt and glacier melt seasons (Figs. ~~3b-c~~3k-l), the stream water samples are clearly located ~~clearly~~ within the triangle formed by the samples of runoff components. The ~~water~~ tracer signatures of glacier meltwater and snowmelt water are similar. The precipitation samples are farther away from the stream water samples compared to the meltwater and groundwater samples. The stream water samples are located nearly in the middle between the meltwater and groundwater samples. This indicates that the contribution of rainfall to total runoff is smallest and the contributions of meltwater and groundwater are similar, in the melt seasons. ~~We assume the tracer signatures of rainfall are represented by the measurements of precipitation samples in all three seasons.~~

4.2 Contributions of runoff components estimated by the mixing approaches

Table 4 and Fig. 4 compare the CRC estimated by ~~multiple~~the mixing approaches. In the cold season (Fig. 4a), the ~~TEMMA~~EMMA_3 estimated the mean contributions of groundwater and snowmelt as 83% and 17%, respectively. The mean contribution of rainfall is

Formatted: German (Germany)

Formatted: German (Germany)

Formatted: German (Germany)

Formatted: German (Germany)

zero. The mean contributions of groundwater, snowmelt and rainfall were estimated as 86% (87%), 13% (12%) and 1% (1%) by the Bayesian_3_OHind (Bayesian_3_~~Cor~~OHcor) approach. As shown in Fig. ~~3a~~3j, the~~ water~~ tracer signature of stream water in this season is close to that of groundwater, while obviously different from that of rainfall. Meanwhile, the stream water samples are outside of the triangle formed by the runoff components, leading to the zero contribution of the rainfall estimated by the ~~TEMMA_3. The ranges for the CRC indicate the uncertainty in the estimates associated with the corresponding mixing approaches (Table 4). The TEMMA_3 produced the highest uncertainty for the CRC, followed by the Bayesian_3. The Bayesian_3_Cor slightly reduced the uncertainty compared to the Bayesian_3, benefiting from the consideration of the correlation between δ^{18}O and δ^{2}H.~~EMMA_3.

In the snowmelt season (Fig. 4b and Table 4), the ~~TEMMA~~EMMA_3 estimated the mean contributions of groundwater, rainfall and snowmelt as 44%, 36% and 20%, respectively. The Bayesian_3_OHind estimated similar mean CRC to ~~the TEMMA~~EMMA_3, whereas the Bayesian_3_~~Cor~~OHcor delivered a lower contribution of snowmelt (32%). When treating the glacier melt and snowmelt as one end-member (i.e. meltwater) in the glacier melt season (Fig. 4c), the ~~TEMMA~~EMMA_3 estimated the mean contributions of groundwater, meltwater and rainfall ~~of~~as 45%, 46% and 9%, respectively. The Bayesian_3_OHind and Bayesian_3_~~Cor~~OHcor estimated a lower contribution of groundwater (43-44%) and a higher contribution of rainfall (11%) compared to ~~the TEMMA~~EMMA_3. ~~In general, the TEMMA_3 estimated the largest~~ The ranges and *Sd* values of CRC in Table 4 indicate the uncertainty ~~for~~in the estimates associated with the corresponding mixing approaches, showing that the ~~contributions~~EMMA_3 produced the highest uncertainty in CRC in all the three seasons, followed by ~~the~~ Bayesian_3_OHind. The Bayesian_3_~~Cor~~OHcor slightly reduced the uncertainty ~~ranges~~ compared to ~~the~~ Bayesian_3~~ (Table 4).~~ _OHind, benefiting from the consideration of the correlation between δ^{18}O and δ^{2}H.

When treating glacier melt and snowmelt as two separate end-members in the glacier melt seasons (Fig. 4d), the ~~TEMMA~~EMMA_4 failed to separate the hydrograph in the glacier melt season, given the large uncertainty range ~~for~~in the contributions of snowmelt and rainfall (0-100%). The tracer signatures of snow and glacier meltwater are rather close to each other, that violates the second assumption of the ~~TEMMA~~EMMA (see Sec. 3.1). In contrast, the Bayesian_4_~~Cor~~OHcor and Bayesian_4_OHind estimated the shares of glacier melt and snowmelt as 25-24% and 21-25%, respectively. Considering the significant snow cover area in September in the study basin (He et al. 2018; He et al. 2019), the contribution of snowmelt in the glacier melt season should be ~~much~~ higher than zero. Again, the Bayesian_4_~~Cor~~OHcor produced smaller uncertainty ranges and *Sd* values for the contributions of groundwater and meltwater compared to ~~the~~ Bayesian_4_OHind and ~~TEMMA~~EMMA_4 (Table 4).

The posterior distributions of ~~water~~ tracer signatures estimated by the Bayesian_4_~~Cor~~OHcor in the glacier melt season are compared with the measured ~~distributions~~histograms of ~~water tracers~~tracer signatures in Fig. 5. The Bayesian_4_~~Cor~~OHcor generally produced similar distributions of water isotopes to the measured distributions, in terms of the similar mean values. The estimated posterior *Sd* values of the water isotopes are smaller than ~~those~~*Sd* values of the ~~measured water isotopes.~~measurements. This can be explained by the incorporation of prior distributions by the Bayesian_4_~~Cor~~OHcor, thus reducing the variability of water isotopes. The posterior *Sd* values for ~~the~~ EC of water sources are also smaller than the measured *Sd* values. However, the posterior distributions of EC show some deviations from the distributions of measured EC~~,~~ (Figs. 5k-o), partly due to the very small sample sizes (see Table 1). The comparison between the posterior distributions of ~~water tracers~~tracer signatures estimated by the Bayesian_3_~~Cor~~OHcor and the measured distributions in the other seasons generally shows a similar behavior (not shown for brevity).

The Bayesian_4_OHind estimated similar posterior distributions of ~~water~~ tracer signatures to the Bayesian_4_~~Cor~~OHcor (except the glacier melt isotopes, Fig. 6), with similar mean tracer values and *Sd*. It is noted that the Bayesian_4_~~Cor~~OHcor estimated smaller *Sd* values for most water sources than the Bayesian_4_OHind (e.g., Figs. 6f-g and 6i-j). Benefiting from the prior information and the consideration of the correlation between $\delta^{18}O$ and $\delta^{2}H$, the Bayesian_4_~~Cor~~OHcor tended to produce the smallest variability in the posterior ~~water tracers~~tracer signatures among all the mixing approaches (Figs. 5-6), thus resulting in the smallest uncertainty for CRC (Fig. 4d). Figure 7 compares the correlation between $\delta^{18}O$ and $\delta^{2}H$ ~~in~~of the measured tracers and the posterior estimates by ~~the~~ Bayesian approaches. The Bayesian_4_~~Cor~~OHcor reproduced the correlation between $\delta^{18}O$ and $\delta^{2}H$ well in comparison to the measured data, whereas the Bayesian_4_OHind failed to capture the correlation.

4.3 Uncertainty ~~for~~of hydrograph separation caused by sampling uncertainty of meltwater

Figure 8 shows the sensitivity of the Bayesian_3_~~Cor~~OHcor and ~~TEMMA~~EMMA_3 approaches to the sampled $\delta^{18}O$ of meltwater in the glacier melt season. The mean CRC quantified by the two mixing approaches ~~show~~shows minor sensitivity to the sample size (scenario I). However, the uncertainty ranges ~~for the~~of contributions tend to decrease with increasing sample size, especially for ~~the TEMMA~~EMMA_3. When assuming only two meltwater samples, the ~~TEMMA~~EMMA_3 resulted in very large uncertainty ranges (0-

100~~%),~~%, Fig. 8d), due to the very wide confidence interval for the *Sd* at a sample size of two. The mean contributions of groundwater and meltwater estimated by the two mixing approaches decrease with increasing mean δ^{18}O of the adopted meltwater sample (scenario II), while the estimated contribution of rainfall increases with the increasing mean δ^{18}O~~. The variations~~ (Fig. 8k). Variations in the mean CRC quantified by ~~the TEMMA~~EMMA_3 are larger than those estimated by the Bayesian_3_~~Cor. In the TEMMA~~OHcor. Using EMMA_3, both the mean contributions of groundwater and meltwater declined by 9% with the assumed increase of the mean δ^{18}O~~,~~ (Figs. 8e and 8h), and the contribution of rainfall increased by 17%. ~~In the~~Using Bayesian_3_~~Cor~~OHcor, the reduction ~~for the~~of contributions of groundwater and snowmelt are 4% and 7%, respectively, and the increase ~~for the~~of contribution of rainfall is only 11~~%.~~% (Fig. 8k). In scenario III, the uncertainty ranges ~~for the~~of CRC (especially for rainfall, Fig. 8l) increase with increasing *Sd* of the sampled δ^{18}O. Again, the increases in the uncertainty ranges estimated by ~~the TEMMA~~EMMA_3 tend to be larger than those estimated by the Bayesian_3_~~Cor~~OHcor. The sensitivity of the mixing approaches to the sampled EC values of the meltwater are similar to the sensitivity to the sampled δ^{18}O (not shown).

4.4 Effect of isotope fractionation on the hydrograph separation

The changes of δ^{18}O caused by the fractionation effect (referring to ξ^{18}O in Eq. 10) during the mixing process are estimated in Figs. 9a-c. The fractionation has the smallest effect on the δ^{18}O of groundwater, while the largest effect on the δ^{18}O of rainfall. ~~Averagely~~ On average, the δ^{18}O of rainfall ~~was~~ increased by around 2.8‰ through ~~the~~ fractionation~~.~~ in all the three seasons. The CRC estimated by the Bayesian_3_~~Cor_F~~OHcor_Frac and Bayesian_4_~~Cor_F~~OHcor_Frac are compared with those estimated by the Bayesian_3_~~Cor~~OHcor and Bayesian_4_~~Cor~~OHcor in Figs. 9d-f, respectively. The mean contribution of groundwater estimated by the Bayesian_3_~~Cor_F~~OHcor_Frac in the cold season is 9% lower than that estimated by the Bayesian_3_~~Cor~~OHcor (Fig. 9d), while the mean contributions of snowmelt and rainfall are 3% and 5% higher, respectively. The reduction of groundwater contribution is ~~the compensation for~~compensated by the increased contributions of snowmelt and rainfall caused by the fractionation effect. In the snowmelt season, the mean contributions of groundwater and rainfall are 1% and 7% lower (Fig. 9e), while the mean contribution of snowmelt estimated by the Bayesian_3_~~Cor_F~~OHcor_Frac is 8% higher. In the glacier melt season, the mean contributions of groundwater and meltwater estimated by the Bayesian_4_~~Cor_F~~OHcor_Frac are higher than those estimated by the Bayesian_4_~~Cor~~OHcor (Fig. 9f~~)~~), and are compensated by the 6% lower contribution of rainfall.

The fractionation effect also produced visible changes on the posterior distributions of $\delta^{18}O$ and $\delta^{2}H$ of runoff components (Fig. 10 shows the example in the glacier melt season). The mean isotopic compositions of runoff components are increased by the fractionation effect. The *Sd* values of the posterior isotopes estimated by the Bayesian_4_~~Cor_F~~OHcor_Frac tend to be higher than those estimated by the Bayesian_4_~~Cor~~OHcor, due to the increased parameter space in the prior assumptions (Eq. 11), thus leading to the larger uncertainty ranges ~~for~~in the contributions of glacier melt and snowmelt (Fig. 9f). As expected, the estimates ~~for the~~of posterior distributions of isotopic compositions of stream water are less sensitive to the fractionation effect of runoff components (Figs. 10e and 10j). The fractionation also has minor effects on the estimates ~~for the~~of posterior distributions of EC values (Figs. 10k-o).

5. Discussion

5.1 Uncertainty ~~for~~of the contributions of runoff components

The ~~TEMMA~~EMMA estimated similar CRCs but with a larger ~~uncertainties for the CRC in comparison to~~uncertainty than the Bayesian approaches. The reasons for this are two-fold. First, the ~~TEMMA~~EMMA estimated the uncertainty ranges ~~for the~~of CRC using the standard deviations (*Sd*) of the measured ~~water~~ tracer signatures. *Sd* ~~is~~values are likely overestimated~~,~~ in this study due to the small sample ~~size~~sizes, and thus insufficiently ~~represents~~representing the variability of the ~~tracers~~tracer signatures of the corresponding water sources~~.~~ across the basin. Due to the limited accessibility of the ~~sampled~~sample sites caused by snow cover, the water samples of meltwater and groundwater are often collected ~~occasionally, thus leading to sharp changes~~sporadically. The small sample size and strong variability in ~~the measured water~~sampled tracer signatures likely led to a large *Sd* value. Second, the ~~TEMMA~~EMMA assumes that the uncertainty associated with each water source is independent from the uncertainty of other water sources (Eq.5), which increases the uncertainty ranges for CRC.

In contrast, the Bayesian approaches estimated smaller variability of ~~water~~ tracer signatures in the posterior distributions compared to the measured ~~water~~ tracer signatures, by updating the prior probability distributions. The posterior distributions were sampled continuously from the assumed value ranges by the MCMC runs, thus reducing the sharp changes and yielding lower variability for the tracer signatures. Moreover, the uncertainty ranges for CRC were quantified using Eqs. 6-10, instead of calculating independently as in the ~~TEMMA~~EMMA. Additionally, the assumed prior distributions ~~for the water tracers~~of tracer signatures and the CRC take into account the correlation between the ~~water tracers~~tracer signatures and the dependence between the runoff components in the Bayesian approaches, thus

Formatted: Font: Italic

resulting in smaller uncertainty ranges (Soulsby et al., 2003). For example, the Bayesian approaches considering the correlation between $\delta^{18}O$ and $\delta^{2}H$ generally estimated smaller uncertainty ranges for CRC compared to those without considering this correlation.

The Gaussian error propagation technique is only capable of considering the uncertainty ~~for the~~of CRC resulting from the variation in the~~ water~~ tracer signatures (Uhlenbrook and Hoeg, 2003). The uncertainty ~~for~~of CRC originated from the sampling uncertainty of meltwater was then investigated in separate virtual sampling experiments. The ~~TEMMA~~EMMA produces large uncertainty ranges and *Sd* values for CRC in the glacier melt season, when the meltwater sample size is rather small. The mean CRC quantified by the ~~TEMMA rely~~EMMA relies more heavily on the mean tracer values of the sampled meltwater, as the mean tracer values are directly used in Eqs. 1-4, in comparison to the mean CRC estimated by the Bayesian approach.

The ~~TEMMA~~EMMA assumes that the~~ water~~ tracer signature of each runoff component is constant during the mixing process, thus is unable to estimate the uncertainty ~~for~~of CRC caused by the isotope fractionation effect. The virtual fractionation experiments using the modified Bayesian approaches show that the isotope fractionation could increase the contribution of snowmelt by 8%, and reduce the contribution of rainfall by 7% in the snowmelt season. We assume the mean CRC estimated by the Bayesian approaches considering the isotope fractionation are more plausible, ~~though~~despite the larger uncertainty ranges. Along the flow path from the source areas to the river channel, the isotopic compositions of meltwater and rainfall are likely increased by the evaporation fractionation effect, especially in the warm seasons. The increased isotopic compositions of meltwater and rainfall during the routing process need to be considered in the mixing approaches for hydrograph separation.

In general, the uncertainty ~~for the~~of CRC is visibly caused by the spatio-temporal variability in the~~ water~~ tracer signatures, the water sampling uncertainty and the isotope fractionation during the mixing process. The uncertainty caused by the water sampling of meltwater tends to be smaller than the uncertainty caused by the variations of the ~~water ~~tracer signatures in both the ~~TEMMA~~EMMA and Bayesian mixing approaches. This is consistent to the findings that the *Sd* values ~~in~~of the tracer measurements of water samples are the main uncertainty sources for the quantification of CRC (Schmieder et al., 2016; Schmieder et al., 2018). The Bayesian approach tends to be superior ~~in~~on narrowing the variability of posterior ~~water~~ tracer signatures benefiting from the prior assumptions and the consideration of the dependence between ~~water ~~tracer signatures and runoff components compared to ~~the TEMMA~~EMMA.

5.2 Limitations

The representativeness of the water samples is one of the limitations of this study. The groundwater was only sampled from a single spring located at the elevation of 2400 m a.s.l, which is rather close to the average altitude of the entire river network in the study basin (2530 m a.s.l.). We thus assume that the measured isotopic composition of the spring water represents the mean isotopic composition of groundwater feeding the river in the basin (~~similarly to~~see also He et al., 2019). Collecting samples from a few ~~spring points~~springs to represent the groundwater end-member has been proposed before (such as Ohlanders et al., 2013 and Mark and McKenzie, 2007), as the accessibility and availability of more potential springs are hampered. Again, for the snow and glacier meltwater samples, we assume that meltwater occurring at similar elevations have similar ~~water~~ tracer signatures (He et al., 2019). The sampled elevation ranges from 1580 m to 4050 m a.s.l., matching with the elevation range where meltwater mainly occurs in the basin (from 1580 m to 3950 m a.s.l.). Considering the isotopic compositions of meltwater are particularly dependent on the elevation, the sampled meltwater could represent meltwater originated from the primary melting locations in the entire basin. The sampled sites thus bear the potential to provide ~~the water~~ tracer signatures ~~for~~of the major ~~share of the~~ meltwater generated in the basin. We ~~divided~~split the entire sampling period (years of 2012 to 2017) into three seasons, i.e. cold season, snowmelt season and glacier melt season, due to the low availability of water samples in each year. By concentrating water samples in the three seasons, we increased the sample sizes of each runoff component for each season, thus increasing the ability of water samples to represent the spatio-temporal variability of seasonal tracer signatures. We used all available groundwater and snowmelt samples from the three seasons for hydrograph separation in the cold season, due to the rather low sample sizes collected in the cold season. This likely leads to overestimated contributions of groundwater and snowmelt in the cold season. However, the overestimation of groundwater contribution is probably small because the tracer signatures of groundwater generally show small seasonal variability. The estimated contributions of snowmelt in the cold season are a bit higher than the contribution modeled by He et al (2018) during DJF (December, January and February), but are still reasonable considering the cold season includes October and November when snow is more prone to melt than DJF.

The assumptions of the mixing approaches lead to another limitation of this study. The ~~TEMMA~~EMMA assumes the tracer signatures of water sources are constant during the mixing process, which is a common assumption for ~~TEMMA.~~the practical application of EMMA. It thus fails to consider the uncertainty originating from the changes of ~~water tracers.~~tracer signatures. In the Bayesian approach, we assumed normal prior distributions for the ~~water~~

~~tracers~~tracer signatures of water sources and Dirichlet prior distribution for the CRC ~~by~~based on literature knowledge (Cable et al., 2011). To refine the description of the temporal and spatial variability of the CRC in the Dirichlet distribution, more hydrological data relating to the runoff processes in the basin are required. We acknowledge that the estimated CRC could be strongly affected by the assumptions of prior distributions. However, testing the effects of the prior assumptions goes beyond the scope of this study. We assume that collecting more water samples from various locations and at different time for each water source could improve the estimation ~~for the~~of tracer signature distributions.

6. Conclusions

This study compared the Bayesian end-member mixing approach with a traditional end-member mixing approach (~~TEMMA~~EMMA) for hydrograph separation in a glacierized basin. The contributions of runoff components (CRC) to the total runoff were estimated for three seasons, i.e. cold season, snowmelt and glacier melt seasons. Uncertainty ~~for~~of these contributions caused by the variability of~~ water~~ tracer signatures, water sampling uncertainty and isotope fractionation were evaluated as follows.

(1) The Bayesian approach generally estimates smaller uncertainty ranges ~~for the~~of CRC, in comparison to the ~~TEMMA~~EMMA. Benefiting from the prior assumptions on~~ water~~ tracer signatures and CRC, as well as from the incorporation of the correlation between tracer signatures in the prior distributions, the Bayesian approach reduced the uncertainty. The Bayesian approach jointly quantified the uncertainty ranges ~~for the~~of CRC. In contrast, the ~~TEMMA~~EMMA estimated the uncertainty ~~for the~~of contribution of each runoff component independently, thus leading to higher uncertainty ranges.

(2) The estimates ~~for~~of CRC in ~~the TEMMA~~EMMA tend to be more sensitive to the sampling uncertainty of meltwater, compared to those in the Bayesian approach. For small sample sizes (e.g., two), ~~the TEMMA~~EMMA estimated very large uncertainty ranges. The mean CRC quantified by ~~the TEMMA~~EMMA are also more sensitive to the mean value of the tracer signature of the meltwater samples than those estimated by the Bayesian approach are.

(3) Ignoring the isotope fractionation during the mixing process likely overestimates the contribution of rainfall and underestimates the contribution of meltwater in the melt seasons. The currently used ~~TEMMA~~EMMA is unable to quantify the uncertainty ~~for~~of CRC caused by the isotope fractionation during the mixing process, due to the underlying assumptions.

Code availability: The R code for the Bayesian end-member mixing approach can be found at https://www.dropbox.com/s/kf2xy3s4vt718s9/Bayesian%20mixing%20approach_four%20components.stan?dl=0

Author contributions.

Conceptualization: Zhihua He, Katy Unger-Shayesteh, and Sergiy Vorogushyn; Data collection: Zhihua He, Katy Unger-Shayesteh, Stephan M. Weise, Olga Kalashnikova, and Abror Gafurov; Methodology: Zhihua He, Katy Unger-Shayesteh, and Sergiy Vorogushyn; Writing original draft: Zhihua He, Sergiy Vorogushyn, and Doris Duethmann: Writing review and editing, All

Competing interests.

The authors declare no conflict of interest.

Acknowledgement

Our work has been funded by the German Federal Ministry for Science and Education (project GlaSCA-V, grant number 88 501) and Volkswagen Foundation (project GlaSCA, grant number 01DK15002A and B), respectively.

Reference

Aizen, V., Aizen, E., Glazirin, G., and Loaiciga, H. A.: Simulation of daily runoff in Central Asian alpine watersheds, Journal of Hydrology, 238, 15-34, https://doi.org/10.1016/S0022-1694(00)00319-X, 2000.

Aizen, V. B., Aizen, E. M., and Melack, J. M.: Precipitation, melt and runoff in the northern Tien Shan, Journal of Hydrology, 186, 229-251, https://doi.org/10.1016/S0022-1694(96)03022-3, 1996.

Aizen, V. B., Kuzmichenok, V. A., Surazakov, A. B., and Aizen, E. M.: Glacier changes in the Tien Shan as determined from topographic and remotely sensed data, Global and Planetary Change, 56, 328-340, https://doi.org/10.1016/j.gloplacha.2006.07.016, 2007.

Barnett, T. P., Adam, J. C., and Lettenmaier, D. P.: Potential impacts of a warming climate on water availability in snow-dominated regions, Nature, 438, 303–309, doi:10.1038/nature04141, 2005.

Beria, H., Larsen, J. R., Michelon, A., Ceperley, N. C., and Schaefli, B.: HydroMix v1.0: a new Bayesian mixing framework for attributing uncertain hydrological sources, Geoscientific Model Development Discussion, https://doi.org/10.5194/gmd-2019-69, in review, 2019.

Brown, L. E., Hannah, D. M., Milner, A. M., Soulsby, C., Hodson, A. J., and Brewer, M. J.: Water source dynamics in a glacierized alpine river basin (Taillon-Gabietous, French Pyrenees), Water Resources Research, 42, W08404, doi:10.1029/2005WR004268, 2006.

Cable, J., Ogle, K., and Williams, D.: Contribution of glacier meltwater to streamflow in the Wind River Range, Wyoming, inferred via a Bayesian mixing model applied to isotopic measurements, Hydrological Processes, 25, 2228-2236, doi:10.1002/hyp.7982, 2011.

Chiogna, G., Santoni, E., Camin, F., Tonon, A., Majone, B., Trenti, A., and Bellin, A.: Stable isotope characterization of the Vermigliana catchment, Journal of Hydrology, 509, 295-305, https://doi.org/10.1016/j.jhydrol.2013.11.052, 2014.

Dahlke, H. E., Lyon, S. W., Jansson, P., Karlin, T., and Rosqvist, G.: Isotopic investigation of runoff generation in a glacierized catchment in northern Sweden, Hydrological Processes, 28, 1383-1398, doi:10.1002/hyp.9668, 2014.

Engel, M., Penna, D., Bertoldi, G., Dell'Agnese, A., Soulsby, C., and Comiti, F.: Identifying run-off contributions during melt-induced run-off events in a glacierized alpine catchment, Hydrological Processes, 30, 343-364, doi:10.1002/hyp.10577, 2016.

Genereux, D.: Quantifying uncertainty in tracer-based hydrograph separations, Water Resources Research, 34, 915-919, https://doi.org/10.1029/98WR00010, 1998.

Gröning, M., Lutz, H.O., Roller-Lutz, Z., Kralik, M., Gourcy, L., and Pöltenstein, L.: A simple rain collector preventing water reevaporation dedicated for $\delta^{18}O$ and $\delta^{2}H$ analysis of cumulative precipitation samples, Journal of Hydrology, 448–449, 195–200, doi: 10.1016/j.jhydrol.2012.04.041, 2012.

He, Z. H., Parajka, J., Tian, F. Q., and Blöschl, G.: Estimating degree-day factors from MODIS for snowmelt runoff modeling, Hydrology and Earth System Sciences, 18, 4773–4789, https://doi.org/10.5194/hess-18-4773-2014, 2014.

He, Z. H., Tian, F. Q., Gupta, H. V., Hu, H. C., and Hu, H. P.: Diagnostic calibration of a hydrological model in a mountain area by hydrograph partitioning, Hydrology and Earth System Sciences, 19, 1807–1826, https://doi.org/10.5194/hess-19-1807-2015, 2015.

He, Z., Unger-Shayesteh, K., Vorogushyn, S., Weise, S. M., Kalashnikova, O., Gafurov, A., Duethmann, D., Barandun, M., and Merz, B.: Constraining hydrological model parameters using water isotopic compositions in a glacierized basin, Central Asia, Journal of Hydrology, 571, 332-348, https://doi.org/10.1016/j.jhydrol.2019.01.048, 2019.

He, Z., Vorogushyn, S., Unger-Shayesteh, K., Gafurov, A., Kalashnikova, O., Omorova, E., and Merz, B.: The Value of Hydrograph Partitioning Curves for Calibrating Hydrological Models in Glacierized Basins, Water Resources Research, 54, 2336-2361, doi.org/10.1002/2017WR021966, 2018.

Joerin, C., Beven, K. J., Iorgulescu, I., and Musy, A.: Uncertainty in hydrograph separations based on geochemical mixing models, Journal of Hydrology, 255, 90-106, https://doi.org/10.1016/S0022-1694(01)00509-1, 2002.

Klaus, J., and McDonnell, J. J.: Hydrograph separation using stable isotopes: Review and evaluation, Journal of Hydrology, 505, 47-64, https://doi.org/10.1016/j.jhydrol.2013.09.006, 2013.

Kong, Y. L., and Pang, Z. H.: Evaluating the sensitivity of glacier rivers to climate change based on hydrograph separation of discharge, Journal of Hydrology, 434, 121-129, https://doi.org/10.1016/j.jhydrol.2012.02.029, 2012.

La Frenierre, J., and Mark, B. G.: A review of methods for estimating the contribution of glacial meltwater to total watershed discharge, Progress in Physical Geography, 38, 173-200, doi:10.1177/0309133313516161, 2014.

Li, Z. X., Feng, Q., Liu, W., Wang, T. T., Cheng, A. F., Gao, Y., Guo, X. Y., Pan, Y. H., Li, J. G., Guo, R., and Jia, B.: Study on the contribution of cryosphere to runoff in the cold alpine basin: A case study of Hulugou River Basin in the Qilian Mountains, Global and Planetary Change, 122, 345-361, https://doi.org/10.1016/j.gloplacha.2014.10.001, 2014.

Mark, B. G., and Mckenzie, J. M.: Tracing increasing tropical Andean glacier melt with stable isotopes in water, Environmental Science & Technology, 41, 6955-6960, https://doi.org/10.1021/es071099d, 2007.

Maurya, A. S., Shah, M., Deshpande, R. D., Bhardwaj, R. M., Prasad, A., and Gupta, S. K.: Hydrograph separation and precipitation source identification using stable water isotopes and conductivity: River Ganga at Himalayan foothills, Hydrological Processes, 25, 1521-1530, doi:10.1002/hyp.7912, 2011.

Moore, J. W., and Semmens, B. X.: Incorporating uncertainty and prior information into stable isotope mixing models, Ecology Letters, 11, 470-480, doi:10.1111/j.1461-0248.2008.01163.x, 2008.

Ohlanders, N., Rodriguez, M., and McPhee, J.: Stable water isotope variation in a Central Andean watershed dominated by glacier and snowmelt, Hydrology and Earth System Sciences, 17, 1035-1050, doi:10.5194/hess-17-1035-2013, 2013.

Parnell, A. C., Inger, R., Bearhop, S., and Jackson, A. L.: Source Partitioning Using Stable Isotopes: Coping with Too Much Variation, PLoS ONE 5(3): e9672. doi:10.1371/journal.pone.0009672, doi:10.1371/journal.pone.0009672, 2010.

Penna, D., Engel, M., Bertoldi, G., and Comiti, F.: Towards a tracer-based conceptualization of meltwater dynamics and streamflow response in a glacierized catchment, Hydrology and Earth System Sciences, 21, 23-41, doi:10.5194/hess-21-23-2017, 2017.

Penna, D., Engel, M., Mao, L., Dell'Agnese, A., Bertoldi, G., and Comiti, F.: Tracer-based analysis of spatial and temporal variations of water sources in a glacierized catchment, Hydrology and Earth System Sciences, 18, 5271-5288, doi:10.5194/hess-18-5271-2014, 2014.

Penna, D., van Meerveld, H. J., Zuecco, G., Fontana, G. D., and Borga, M.: Hydrological response of an Alpine catchment to rainfall and snowmelt events, Journal of Hydrology, 537, 382-397, https://doi.org/10.1016/j.jhydrol.2016.03.040, 2016.

Pohl, E., Gloaguen, R., Andermann, C., and Knoche, M.: Glacier melt buffers river runoff in the Pamir Mountains, Water Resources Research, 53, 2467-2489, doi:10.1002/2016WR019431, 2017.

Pu, T., He, Y. Q., Zhu, G. F., Zhang, N. N., Du, J. K., and Wang, C. F.: Characteristics of water stable isotopes and hydrograph separation in Baishui catchment during the wet season in Mt.Yulong region, south western China, Hydrological Processes, 27, 3641-3648, doi: 10.1002/hyp.9479, 2013.

Pu, T., Qin, D. H., Kang, S. C., Niu, H. W., He, Y. Q., and Wang, S. J.: Water isotopes and hydrograph separation in different glacial catchments in the southeast margin of the Tibetan Plateau, Hydrological Processes, 31, 3810-3826, doi:10.1002/hyp.11293, 2017.

Rahman, K., Besacier-Monbertrand, A. L., Castella, E., Lods-Crozet, B., Ilg, C., and Beguin, O.: Quantification of the daily dynamics of streamflow components in a small alpine watershed in Switzerland using end member mixing analysis, Environmental Earth Sciences, 74, 4927-4937, https://doi.org/10.1007/s12665-015-4505-5, 2015.

Schmieder, J., Garvelmann, J., Marke, T., and Strasser, U.: Spatio-temporal tracer variability in the glacier melt end-member How does it affect hydrograph separation results, Hydrological Processes, 32, 1828-1843, doi:10.1002/hyp.11628, 2018.

Schmieder, J., Hanzer, F., Marke, T., Garvelmann, J., Warscher, M., Kunstmann, H., and Strasser, U.: The importance of snowmelt spatiotemporal variability for isotope-based hydrograph separation in a high-elevation catchment, Hydrology and Earth System Sciences, 20, 5015-5033, doi:10.5194/hess-20-5015-2016, 2016.

Soulsby, C., Petry, J., Brewer, M. J., Dunn, S. M., Ott, B., and Malcolm, I. A.: Identifying and assessing uncertainty in hydrological pathways: a novel approach to end member mixing in a Scottish agricultural catchment, Journal of Hydrology, 274, 109-128, https://doi.org/10.1016/S0022-1694(02)00398-0, 2003.

Sun, C. J., Chen, Y. N., Li, W. H., Li, X. G., and Yang, Y. H.: Isotopic time series partitioning of streamflow components under regional climate change in the Urumqi River, northwest China, Hydrological Sciences Journal-Journal Des Sciences Hydrologiques, 61, 1443-1459, doi:10.1080/02626667.2015.1031757, 2016a.

Sun, C. J., Yang, J., Chen, Y. N., Li, X. G., Yang, Y. H., and Zhang, Y. Q.: Comparative study of streamflow components in two inland rivers in the Tianshan Mountains, Northwest China, Environmental Earth Sciences, 75:727. doi:10.1007/s12665-016-5314-1, 2016b.

Uhlenbrook, S., and Hoeg, S.: Quantifying uncertainties in tracer-based hydrograph separations: a case study for two-, three- and five-component hydrograph separations in a mountainous catchment, Hydrological Processes, 17, 431-453, doi:10.1002/hyp.1134 2003.

Viviroli, D., Durr, H. H., Messerli, B., Meybeck, M., and Weingartner, R.: Mountains of the world, water towers for humanity: Typology, mapping, and global significance, Water Resources Research, 43, W07447, https://doi.org/10.1029/2006wr005653, 2007.

Ward, E. J., Semmens, B. X., and Schindler, D. E.: Including Source Uncertainty and Prior Information in the Analysis of Stable Isotope Mixing Models, Environmental Science & Technology, 44, 4645-4650, doi:10.1021/es100053v, 2010.

Formatted: English (United States)

Formatted: English (United States)

Formatted: English (United States)

LIST OF TABLES

Formatted: English (United States)

Table 1. ~~Water tracer~~Tracer signatures measured from water samples in three seasons. ~~CV is the ratio between the standard deviation and mean value~~CV stands for coefficient of variation.

Season	Water source	Tracer	Sample size	Mean	Range	CV
Cold season (October to February)	Groundwater	^{18}O (δ,‰)	23	-11.37	(-12.12, -10.61)	0.04
		^{2}H (δ,‰)	23	-73.~~9~~90	(-77.~~9~~90, -68.~~2~~20)	0.03
		EC(μs/cm)	13	126.~~8~~80	(69.~~6~~60, 167.~~2~~20)	0.24
	Precipitation	^{18}O (δ,‰)	37	-15.93	(-22.82, -7.70)	0.21
		^{2}H (δ,‰)	37	-111.~~5~~50	(-168.~~8~~80, -39.~~1~~10)	0.27
		EC(μs/cm)	23	67.~~8~~80	(21.~~3~~30, 99.~~6~~60)	0.34
	Snowmelt	^{18}O (δ,‰)	36	-12.51	(-17.31, -6.95)	0.19
		^{2}H (δ,‰)	36	-84.~~6~~60	(-120.~~7~~70, -38.~~7~~70)	0.23
		EC(μs/cm)	15	53.~~7~~70	(8.~~8~~80, 151.00)	0.96
	Stream water	^{18}O (δ,‰)	150	-11.33	(-11.82, -9.05)	0.03
		^{2}H (δ,‰)	150	-74.~~2~~20	(-77.~~5~~50, -68.~~2~~20)	0.03
		EC(μs/cm)	90	112.~~2~~20	(80.~~3~~30, 139.~~3~~30)	0.13

Table 1 Continued.

Season	Water source	Tracer	Sample size	Mean	Range	CV
Snowmelt season (March to June)	Groundwater	^{18}O (δ,‰)	9	-11.34	(-11.94, -11.06)	0.02
		^{2}H (δ,‰)	9	-73.~~9~~90	(-77.~~3~~30, -72.~~4~~40)	0.02
		EC(μs/cm)	8	133.~~1~~10	(94.00, 167.~~2~~20)	0.21
	Precipitation	^{18}O (δ,‰)	25	-7.89	(-16.81, -0.06)	0.46
		^{2}H (δ,‰)	25	-49.~~2~~20	(-120.~~5~~50, -3.~~9~~90)	0.52
		EC(μs/cm)	11	58.~~3~~30	(25.~~8~~80, 84.~~3~~30)	0.34
	Snowmelt	^{18}O (δ,‰)	15	-13.87	(-16.74, -10.96)	0.11
		^{2}H (δ,‰)	15	-95.~~9~~90	(-119.~~3~~30, -70.~~5~~50)	0.13
		EC(μs/cm)	11	67.~~3~~30	(11.~~0~~00, 151.~~0~~00)	0.80
	Stream water	^{18}O (δ,‰)	126	-11.58	(-12.91, -10.04)	0.04
		^{2}H (δ,‰)	126	-76.~~1~~10	(-86.~~4~~40, -67.~~0~~00)	0.04
		EC(μs/cm)	23	94.~~9~~90	(80.~~1~~10, 114.~~0~~00)	0.09
~~Glacier melt season (July to September)~~	~~Groundwater~~	~~^{18}O (δ,‰)~~	~~14~~	~~-11.4~~	~~(-12.12, -10.61)~~	~~0.04~~
		~~^{2}H (δ,‰)~~	~~14~~	~~-73.9~~	~~(-77.9, -68.2)~~	~~0.04~~
		~~EC(μs/cm)~~	~~5~~	~~116.7~~	~~(69.6, 142.6)~~	~~0.30~~

Table 1 Continued.

Season	Water source	Tracer	Sample size	Mean	Range	CV
	Groundwater	^{18}O (δ,‰)	14	-11.40	(-12.12, -10.61)	0.04
		^{2}H (δ,‰)	14	-73.90	(-77.90, -68.20)	0.04
		EC(μs/cm)	5	116.70	(69.60, 142.60)	0.30
	Precipitation	^{18}O (δ,‰)	28	-6.72	(-13.02, 1.51)	0.56
		^{2}H (δ,‰)	28	-42.~~6~~60	(-94.~~9~~90, 3.~~0~~00)	0.58
		EC(μs/cm)	9	67.~~7~~70	(26.~~7~~70, 102.~~0~~00)	0.39
Glacier melt season (July to September)	Snowmelt	^{18}O (δ,‰)	15	-12.70	(-17.31, -9.85)	0.15
		^{2}H (δ,‰)	15	-85.~~6~~60	(-120.~~7~~70, -64.~~0~~00)	0.17
		EC(μs/cm)	4	16.~~2~~20	(8.~~8~~80, 24.~~3~~30)	0.51
	Glacier melt	^{18}O (δ,‰)	23	-13.11	(-14.96, -11.55)	0.10
		^{2}H (δ,‰)	23	-87.~~2~~20	(-100.~~4~~40, -75.~~5~~50)	0.11
		EC(μs/cm)	10	9.~~9~~90	(1.~~5~~50, 33.~~4~~40)	1.28
	Stream water	^{18}O (δ,‰)	119	-11.75	(-12.97, -5.64)	0.07
		^{2}H (δ,‰)	119	-77.~~2~~20	(-86.~~7~~70, -62.~~3~~30)	0.05
		EC(μs/cm)	24	64.~~5~~50	(33.~~4~~40, 99.~~3~~30)	0.25

Table 2. Mixing approaches used for hydrograph separation in different seasons.

Mixing approach	Description	End-member	Used tracers	Seasons applied to
~~TEMMA~~EMMA_3	Three-component traditional end-member mixing approach	Groundwater, snowmelt (or meltwater) and rainfall	^{18}O and EC	Cold season, snowmelt season and glacier melt season
~~TEMMA~~EMMA_4	Four-component traditional end-member mixing approach	Groundwater, snowmelt, glacier melt and rainfall	^{18}O, ^{2}H and EC	Glacier melt season
Bayesian_3_OHind	Three-component Bayesian approach, without considering the correlation between δ^{18}O and δ^{2}H	Groundwater, snowmelt (or meltwater) and rainfall	^{18}O and EC	Cold season, snowmelt season and glacier melt season
Bayesian_3_~~Cor~~OHcor	Three-component Bayesian approach, considering the correlation between δ^{18}O and δ^{2}H	Groundwater, snowmelt (or meltwater) and rainfall	^{18}O, ^{2}H and EC	Cold season, snowmelt season and glacier melt season
Bayesian_3_~~Cor_F~~OHcor_Frac	Three-component Bayesian approach, considering the correlation between δ^{18}O and δ^{2}H and the fractionation of δ^{18}O and δ^{2}H during the mixing process	Groundwater, snowmelt and rainfall	^{18}O, ^{2}H and EC	Cold season and snowmelt season
Bayesian_4_OHind	Four-component Bayesian approach, without considering the correlation between ^{18}O and ^{2}H	Groundwater, snowmelt, glacier melt and rainfall	^{18}O, ^{2}H and EC	Glacier melt season
Bayesian_4_~~Cor~~OHcor	Four-component Bayesian approach, considering the correlation between δ^{18}O and δ^{2}H	Groundwater, snowmelt, glacier melt and rainfall	^{18}O, ^{2}H and EC	Glacier melt season
Bayesian_4_~~Cor_F~~OHcor_Frac	Four-component Bayesian approach, considering the correlation between δ^{18}O and δ^{2}H and the fractionation of δ^{18}O and δ^{2}H during the mixing process	Groundwater, snowmelt, glacier melt and rainfall	^{18}O, ^{2}H and EC	Glacier melt season

Table 3. Parameters used for ~~the~~ prior distributions in the Bayesian approaches.

Parameter	Description	Applied Bayesian approach	Value range	Equation
$\gamma^{18}O$	Mean of the prior normal distributions for the mean $\delta^{18}O$ of runoff components	All Bayesian approaches	(-50,50)	Eq.7a
$\gamma^{2}H$	Mean of the prior normal distributions for the mean $\delta^{2}H$ of runoff components	All Bayesian approaches, except Bayesian_3_OHind	(-200,200)	Eq.7b
$\sigma^{18}O$	Variance of the prior normal distributions for the mean $\delta^{18}O$ of runoff components	All Bayesian approaches	(0,50)	Eq.7a
$\sigma^{2}H$	Variance of the prior normal distributions for the mean $\delta^{2}H$ of runoff components	All Bayesian approaches, except Bayesian_3_OHind	(0,200)	Eq.7b
$\lambda^{18}O$	Variance of the prior normal distributions for the $\delta^{18}O$ of runoff components and stream water	Bayesian_3_OHind and Bayesian_4_OHind	(0,50)	Eq.6c
$\lambda^{2}H$	Variance of the prior normal distributions for the $\delta^{2}H$ of runoff components and stream water	Bayesian_4_OHind	(0,200)	Eq.6d
τ	Variance of the prior normal distributions for the EC of runoff components and stream water	All Bayesian approaches	(0,400)	Eq.8a
θ	Mean of the prior normal distributions for the mean EC of runoff components	All Bayesian approaches	(0,400)	Eq.8b
ω	Variance of the prior normal distributions for the mean EC of runoff components	All Bayesian approaches	(0,400)	Eq.8b
$\boldsymbol{\beta}$	Mean of the prior bivariate normal distributions for parameters descripting the α value in the Dirichlet distribution of contributions of runoff components	All Bayesian approaches	(0,10)	Eq.9d
$\eta^{18}O$	Mean of the prior bivariate normal distributions for the fractionations of $\delta^{18}O$ of runoff components	Bayesian_3_~~Cor_F~~OHcor_Frac and Bayesian_4_~~Cor_F~~OHcor_Frac	(0,5)	Eq.11
$\eta^{2}H$	Mean of the prior bivariate normal distributions for the fractionations of $\delta^{2}H$ of runoff components	Bayesian_3_~~Cor_F~~OHcor_Frac and Bayesian_4_~~Cor_F~~OHcor_Frac	(0,5)	Eq.11

Formatted Table

Table 4. Contributions of runoff components (CRC) estimated by the different mixing approaches ~~(%).~~(percentage, %). The ranges (%) show the difference between the 95% and 5% percentiles. *Sd* values refer to the standard deviations.

	Mixing approach	Groundwater			Snowmelt			Rainfall			Glacier melt	
		Mean	Range	*Sd*	Mean	Range	*Sd*	Mean	Range	*Sd*	Mean	Range
Cold season	~~TEMMA~~EMMA_3	83	41	0.12	17	46	0.17	0	10	0.12	-	-
	Bayesian_3_OHind	86	28	0.01	13	28	0.09	1	3	0.09	-	-
	Bayesian_3_~~Cor~~OHcor	87	24	0.01	12	24	0.07	1	3	0.07	-	-
~~Snowmlet~~Snowmelt season	~~TEMMA~~EMMA_3	44	50	0.15	36	33	0.11	20	25	0.09	-	-
	Bayesian_3_OHind	42	33	0.12	36	22	0.10	22	20	0.07	-	-
	Bayesian_3_~~Cor~~OHcor	46	30	0.12	32	20	0.09	22	19	0.06	-	-
Glacier melt season (three-component)	~~TEMMA~~EMMA_3	45	48	0.13	-	-	-	9	17	0.06	-	-
	Bayesian_3_OHind	43	25	0.11	-	-	-	11	13	0.06	-	-
	Bayesian_3_~~Cor~~OHcor	44	24	0.11	-	-	-	11	12	0.05	-	-
Glacier melt season (four-component)	~~TEMMA~~EMMA_4	45	48	0.14	0	100	0.33	11	100	0.35	44	78
	Bayesian_4_OHind	44	30	0.10	21	42	0.09	10	13	0.13	25	41
	Bayesian_4_~~Cor~~OHcor	41	23	~~-~~0.10	25	33	~~-~~0.07	10	13	~~-~~0.10	24	33

LIST OF FIGURES

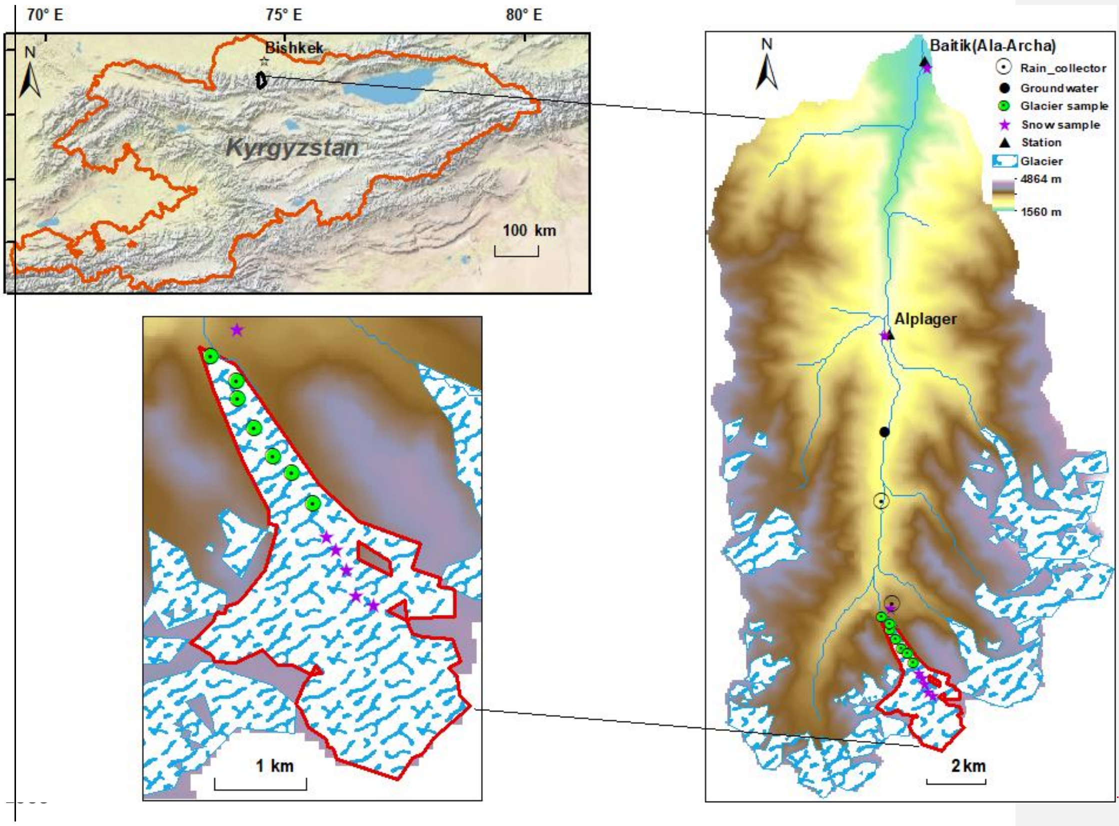
70° E
75° E
80° E
43° N
42° N
41° N
40° N
N
Bishkek
Kyrgyzstan
100 km
1 km
N
Baitik(Ala-Archa)
Rain_collector
Groundwater
Glacier sample
Snow sample
Station
Glacier
4864 m
1560 m
Alplager
2 km

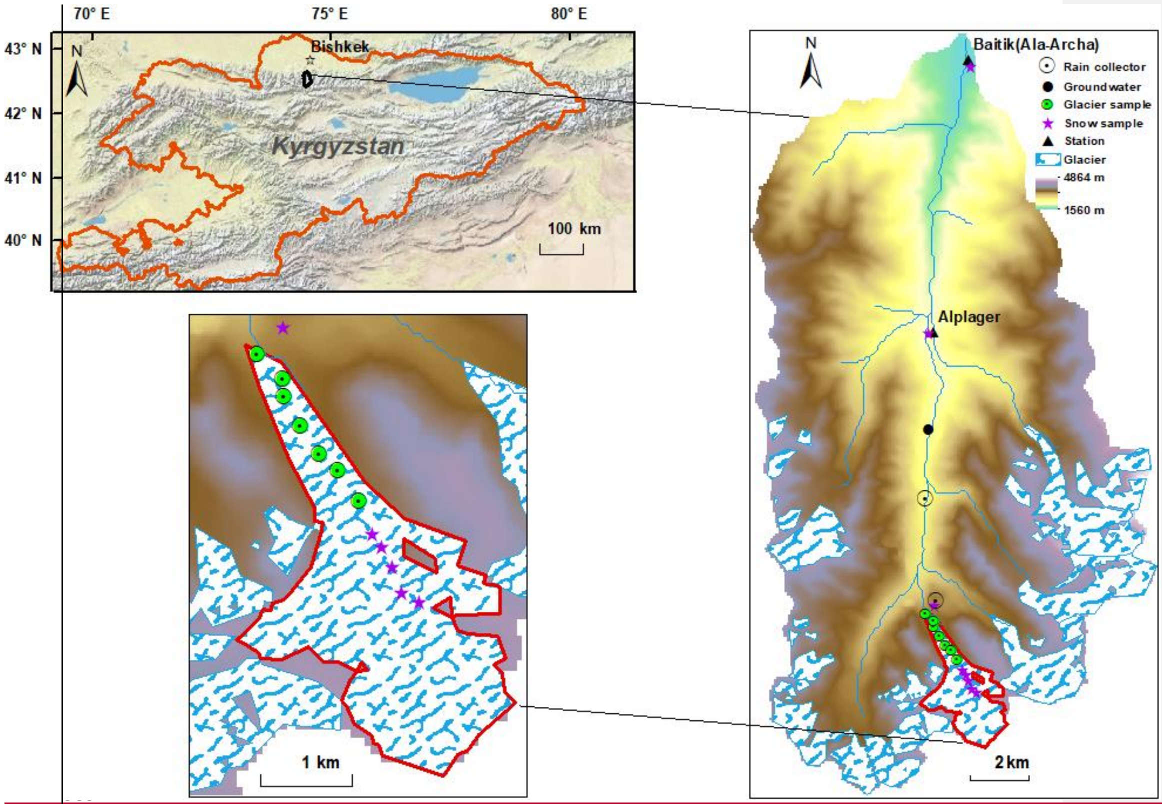

1390 Figure 1. Study area of the Ala-Archa basin (derived from the ESRI World Topographic Map)
1391 and the Golubin Glacier including the locations of the water sampling points.

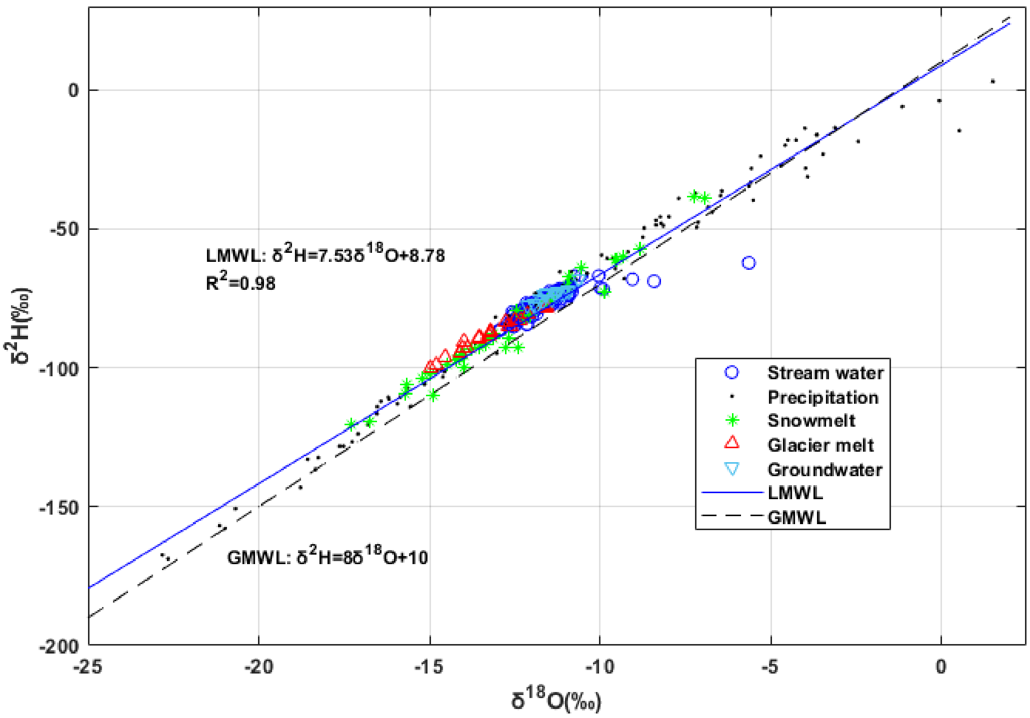

Figure 2. Isotope signatures of water samples from the three seasons in the Ala-Archa basin.

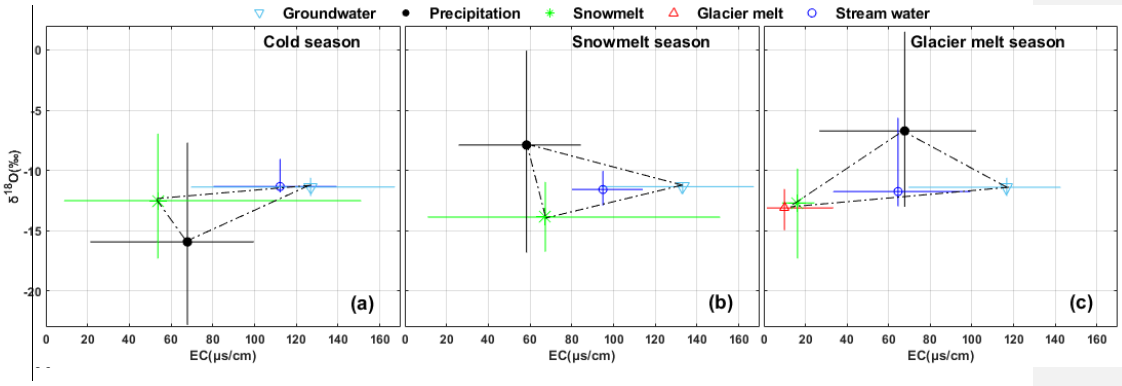

Groundwater
Precipitation
Snowmelt
Glacier melt
Stream water
Cold season
Snowmelt season
Glacier melt season
δ18O(‰)
EC(μs/cm)
(a)
(b)
(c)

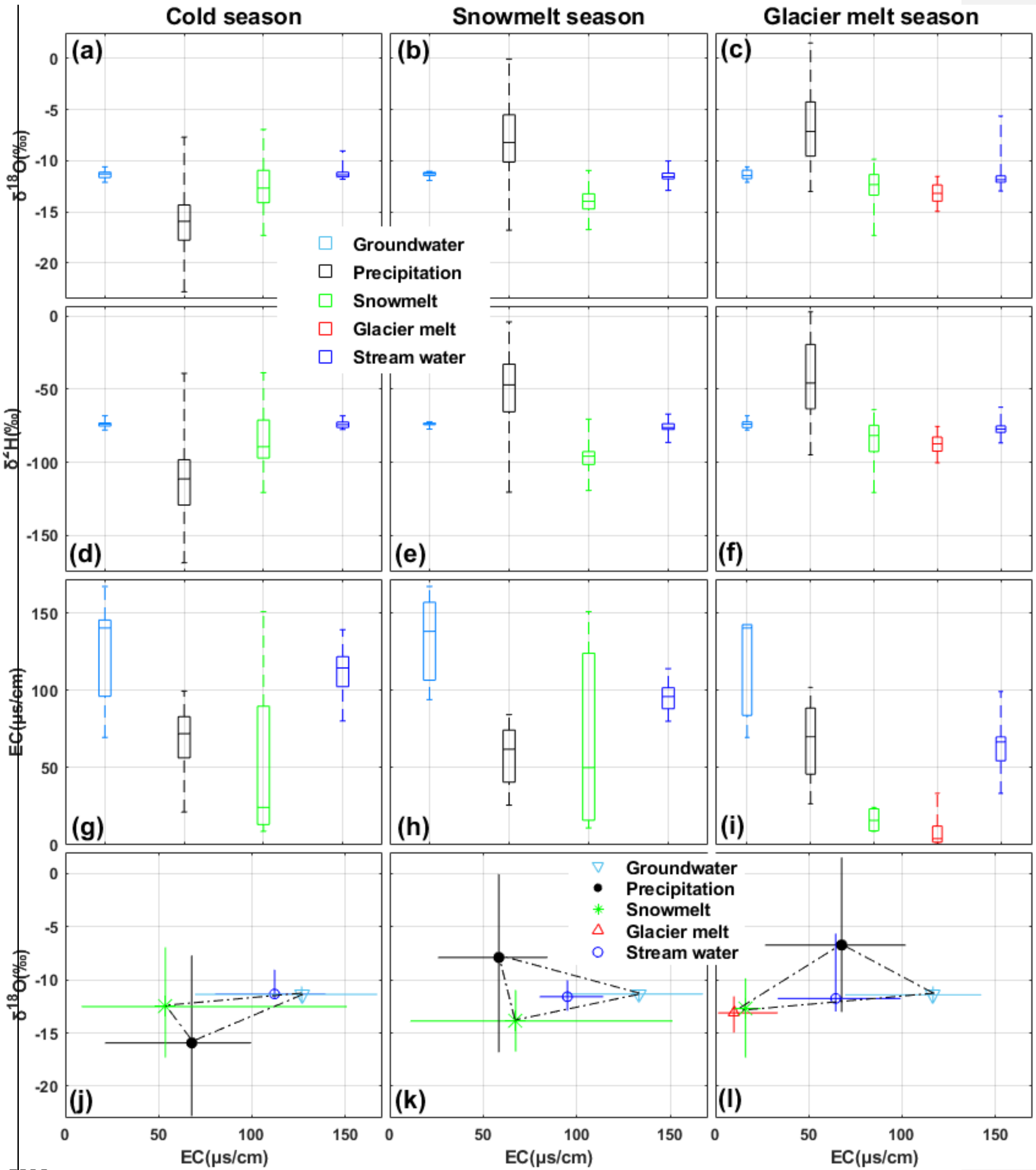

Figure 3. (a)-(i) Boxplots of tracer signatures in three seasons. (j)- (l) δ^{18}O-EC mixing space of the various water sources in the three seasons~~. The~~; the solid lines indicate the ranges of tracer signatures measured from water samples.

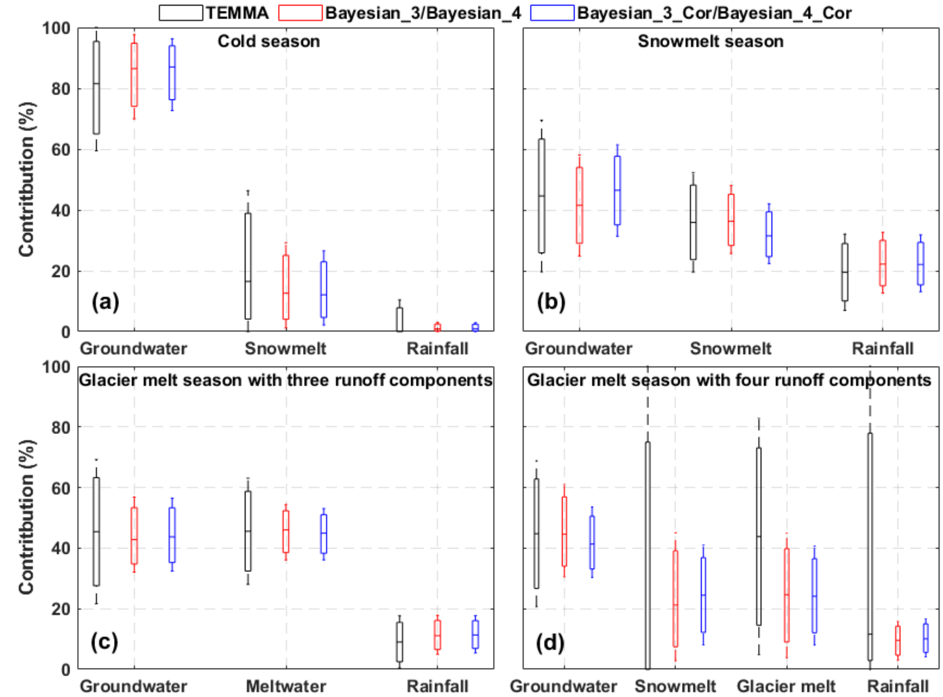
TEMMA
Bayesian_3/Bayesian_4
Bayesian_3_Cor/Bayesian_4_Cor
Cold season
Snowmelt season
Glacier melt season with three runoff components
Glacier melt season with four runoff components
Contritbution (%)
(a)
(b)
(c)
(d)
Groundwater
Snowmelt
Rainfall
Meltwater
Glacier melt
0
20
40
60
80
100

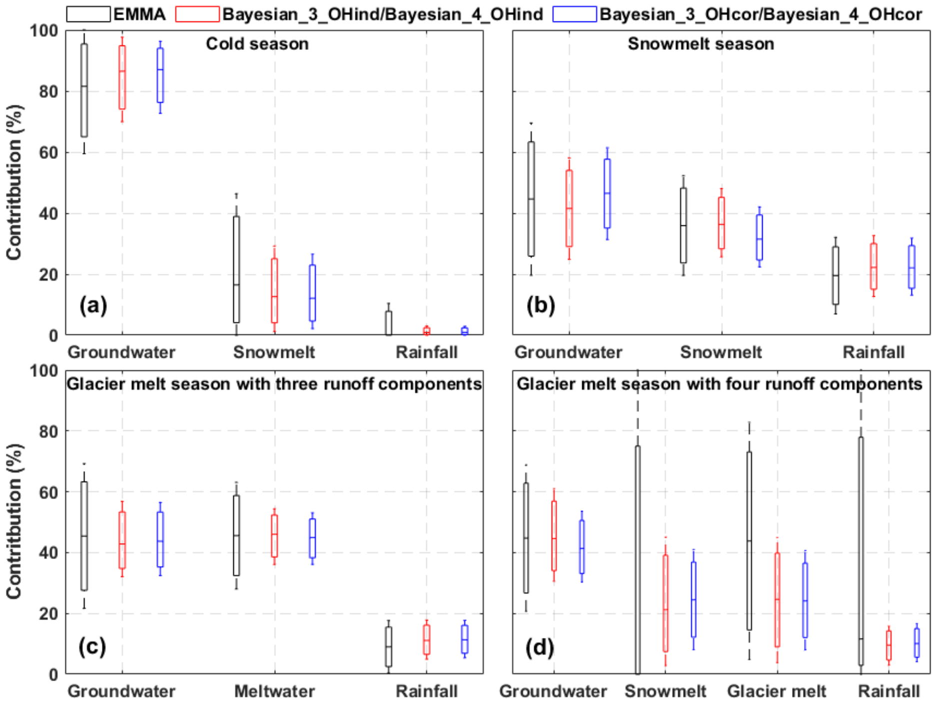
EMMA
Bayesian_3_OHind/Bayesian_4_OHind
Bayesian_3_OHcor/Bayesian_4_OHcor
Cold season
Snowmelt season
Glacier melt season with three runoff components
Glacier melt season with four runoff components
Contritbution (%)
(a)
(b)
(c)
(d)
Groundwater
Snowmelt
Rainfall
Meltwater
Glacier melt
0
20
40
60
80
100

Figure 4. Contributions of runoff components (CRC) to total runoff estimated by different mixing approaches in three seasons. The Bayesian_3_OHind and Bayesian_3_~~Cor~~OHcor were applied in the ~~clod~~cold and melt seasons (a-c), and the Bayesian_4_OHind and Bayesian_4_~~Cor~~OHcor were applied in the glacier melt season (d). The horizontal lines in the boxes refer to the median contributions, and whiskers refer to the 95% and 5% percentiles.

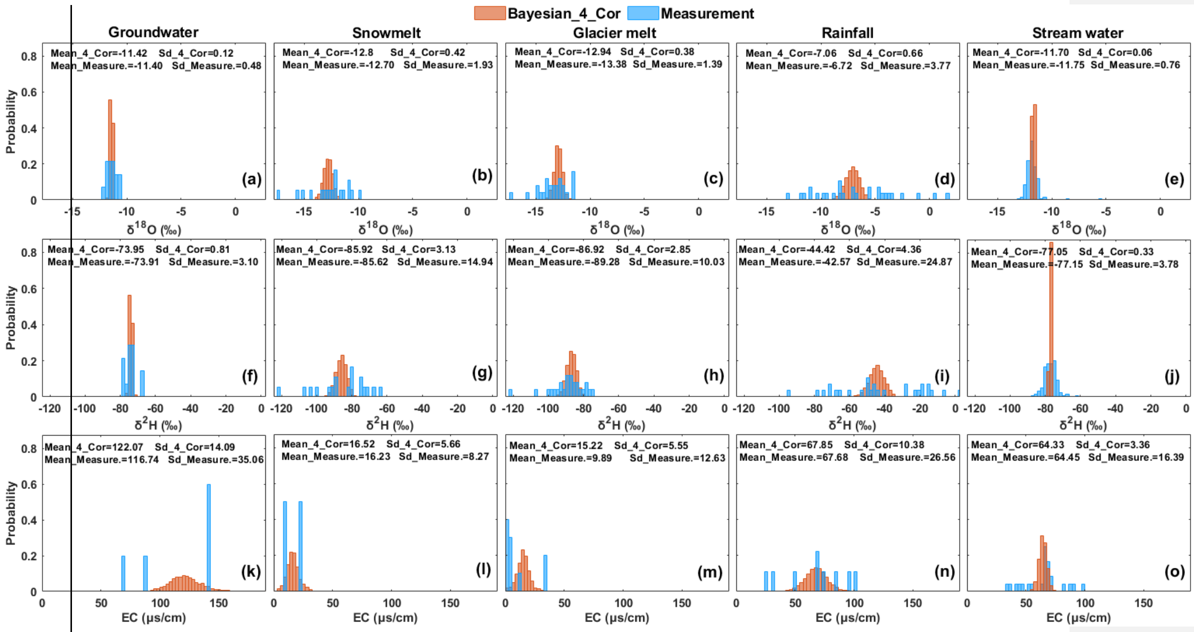

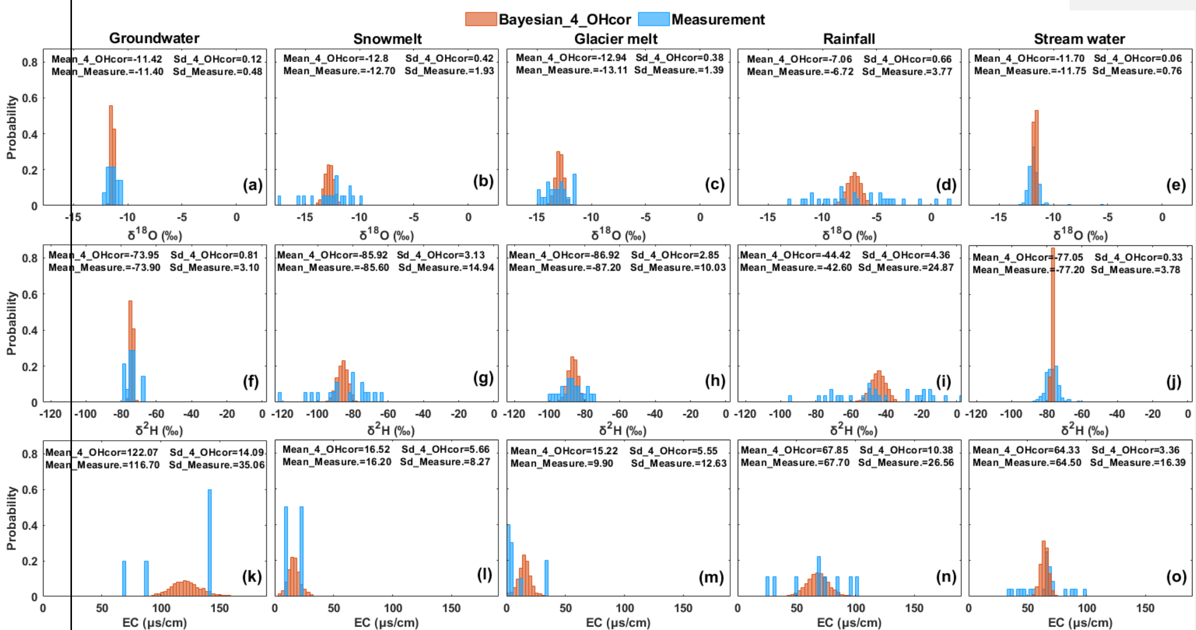

Figure 5. Posterior distributions of ~~water~~ tracer signatures estimated by the Bayesian_4_~~Cor~~OHcor in the glacier melt season. Measurement refers to the distributions of

~~water~~ tracer signatures from the water samples. Row 1: distributions of $\delta^{18}O$; Row 2: distributions of $\delta^{2}H$; Row 3: distributions of EC.

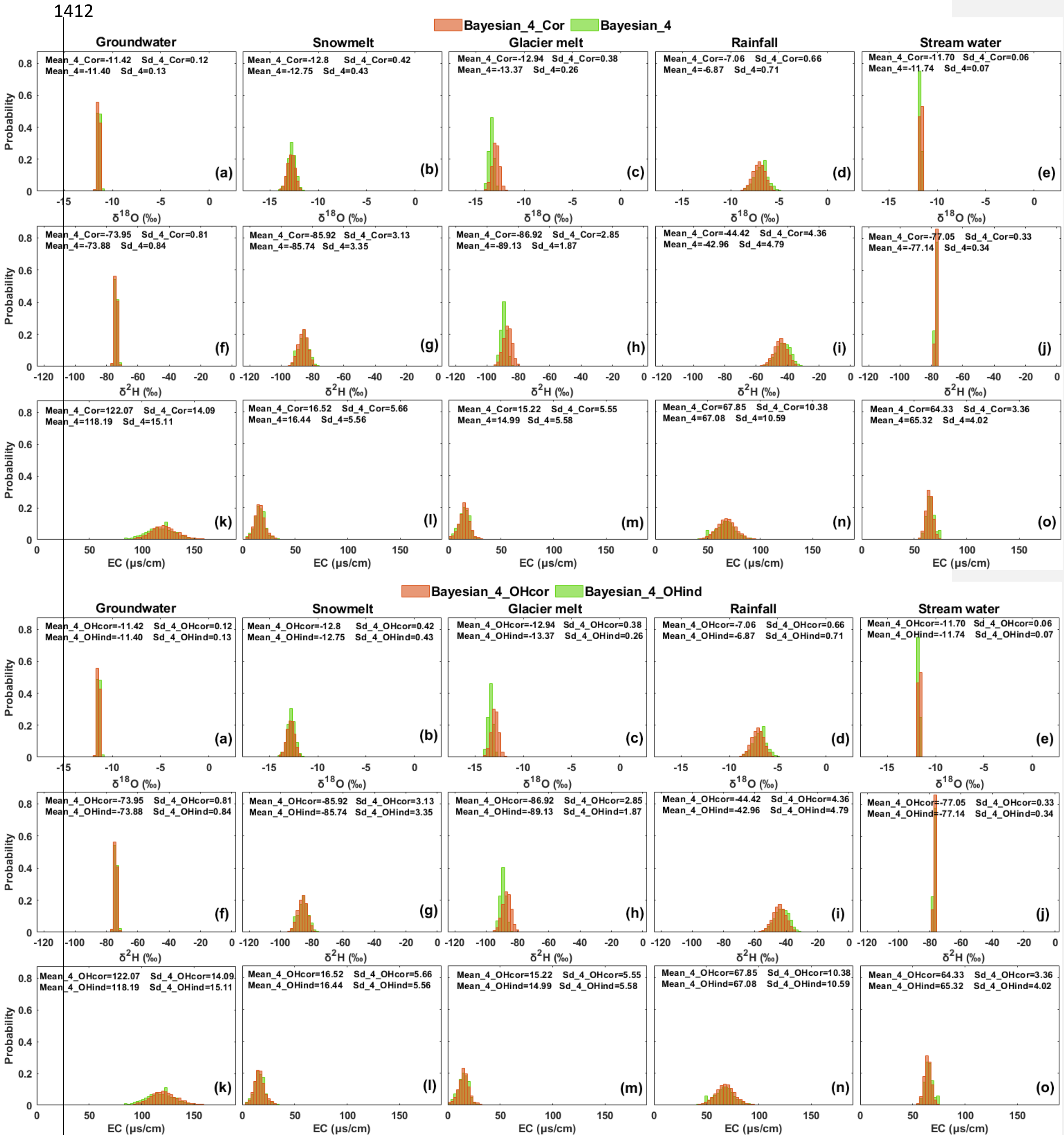

Figure 6. Comparison of the posterior distributions of ~~water tracers~~tracer signatures estimated by the Bayesian approaches with (Bayesian_4_~~Cor~~OHcor) and without (Bayesian_4_OHind) considering the correlation between $\delta^{18}O$ and $\delta^{2}H$ in the glacier melt season.

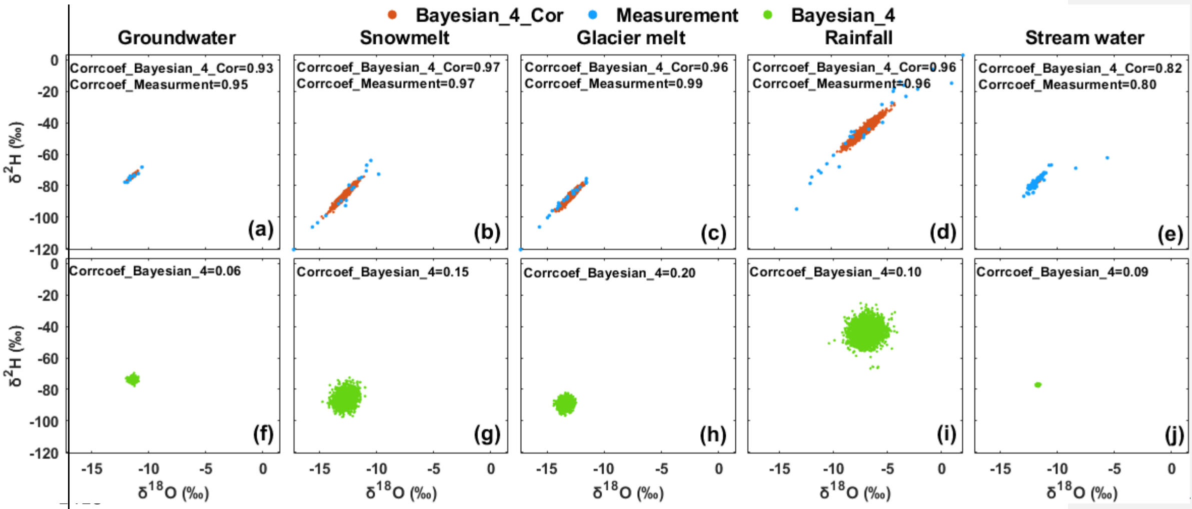

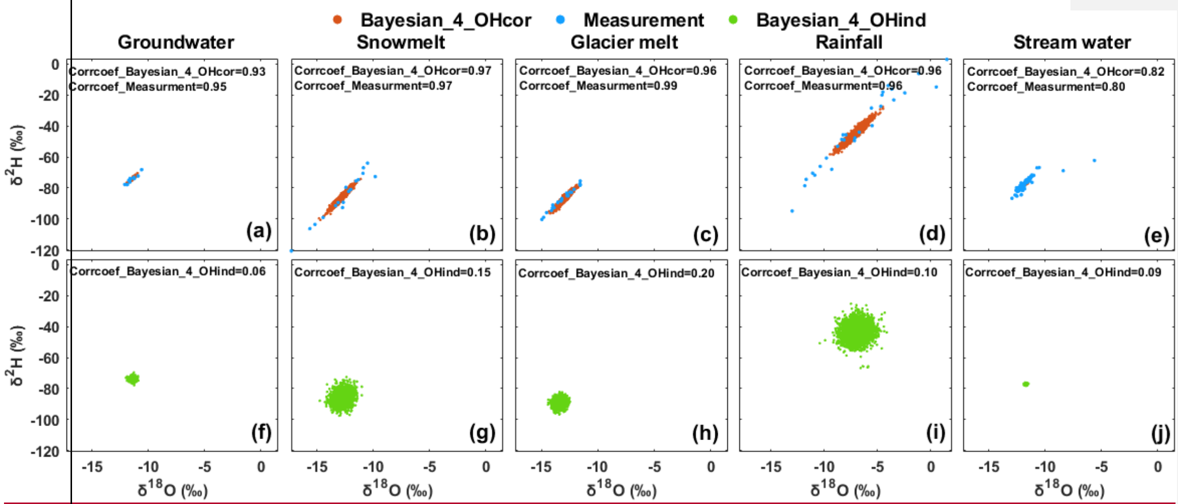

Figure 7. Correlation between posterior $\delta^{18}O$ and $\delta^{2}H$ estimated by the Bayesian_4_~~Cor~~OHcor and the Bayesian_4_OHind approaches in the glacier melt season.

1422

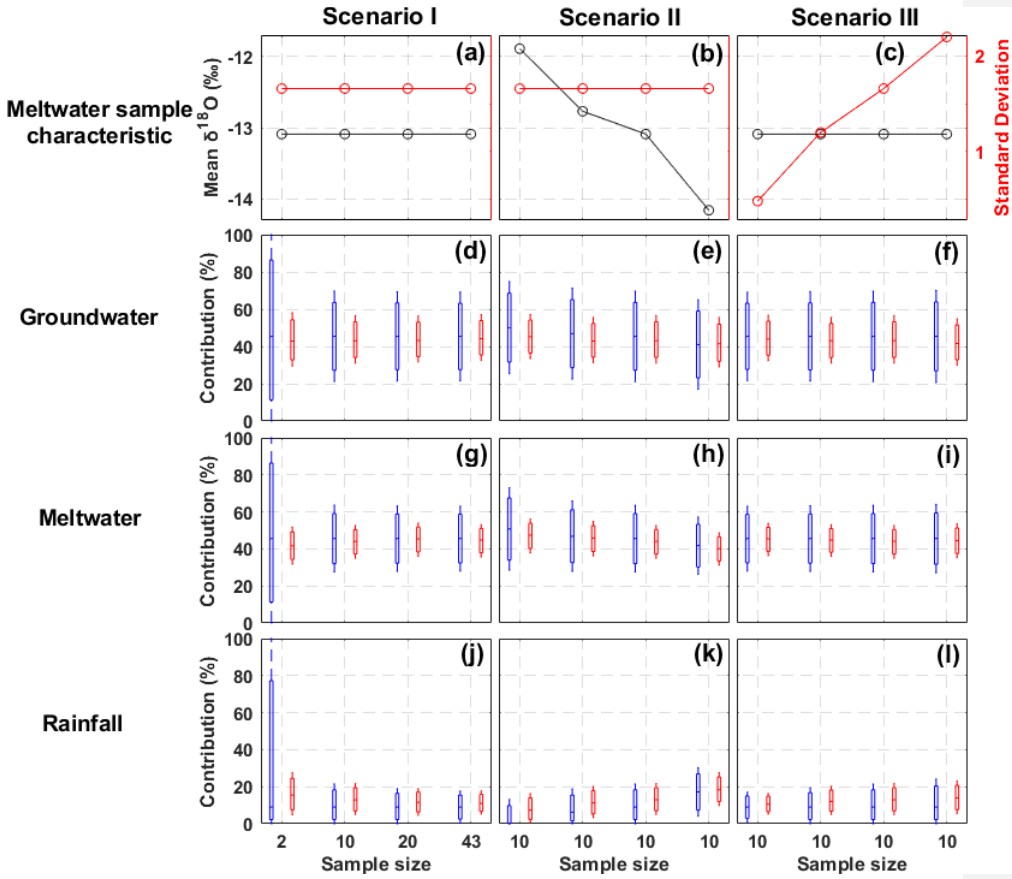

Scenario I
Scenario II
Scenario III
Meltwater sample characteristic
Groundwater
Meltwater
Rainfall
Mean δ18O (‰)
Standard Deviation
Contribution (%)
(a)
(b)
(c)
(d)
(e)
(f)
(g)
(h)
(i)
(j)
(k)
(l)
Sample size

1423

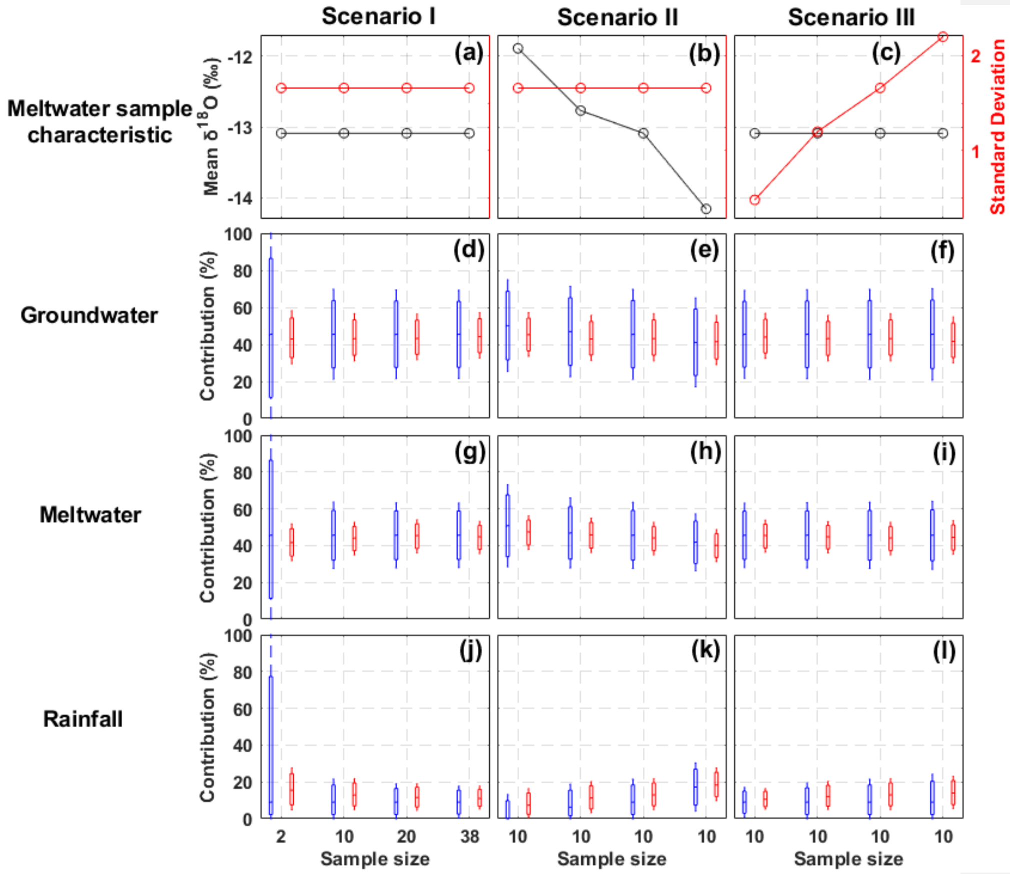

Figure 8. Sensitivity of the CRC estimates ~~for CRC~~ to the sample size (Scenario I), the mean (Scenario II) and standard deviation (Scenario III) of $\delta^{18}O$ of meltwater in the glacier melt season. Red boxes show the contributions estimated by the Bayesian_3_~~Cor~~OHcor, and the blue boxes refer to the contributions estimated by the ~~TEMMA~~EMMA_3.

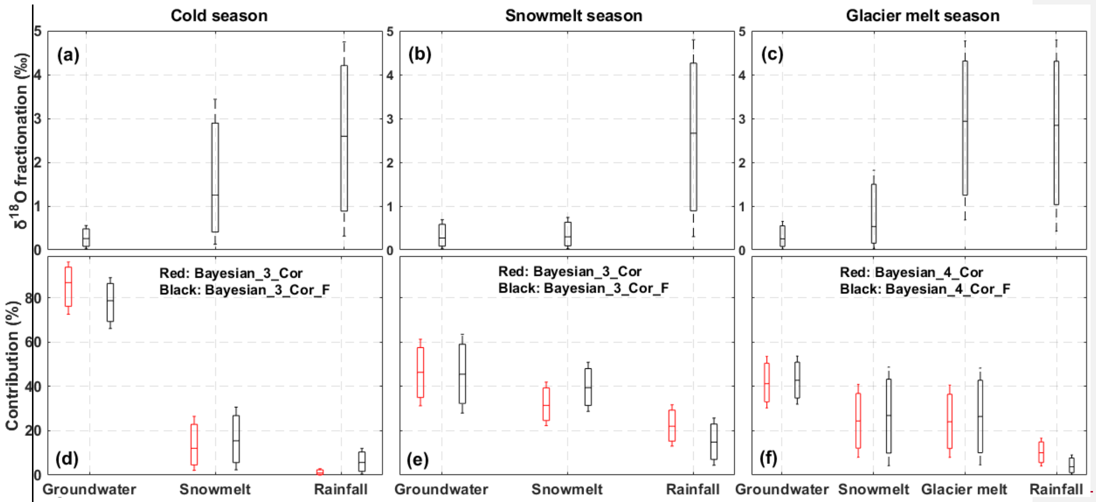

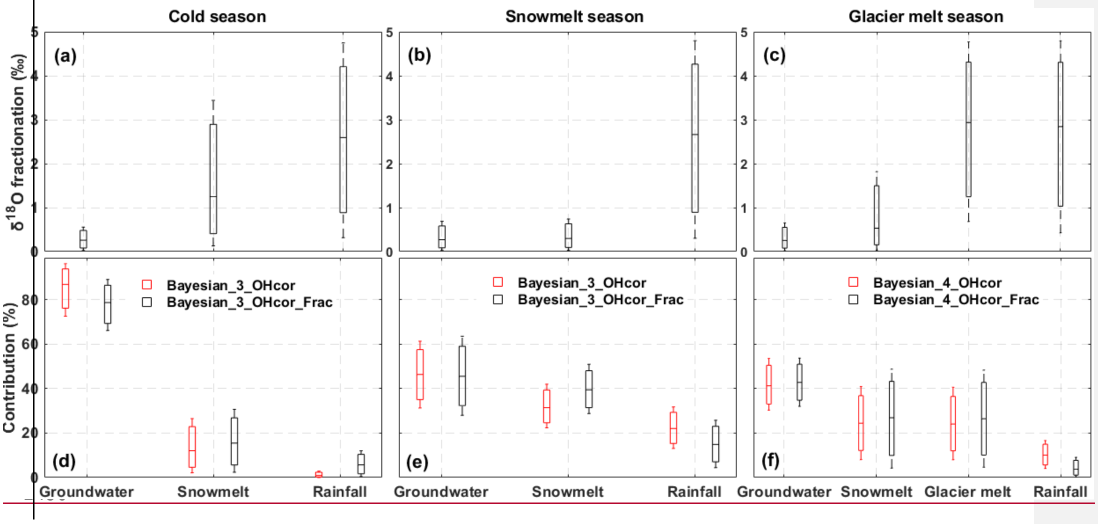

Figure 9. Effects of isotope fractionation on the estimates of CRC in the Bayesian approach for the three seasons. (a)-(c): Estimated changes in $\delta^{18}O$ of runoff components caused by the fractionation effect; (d)-(e): Comparison of the CRC estimated by the Bayesian_3_~~Cor~~OHcor and the Bayesian_3_~~Cor_F~~OHcor_Frac; (f): Comparison of the CRC estimated by the Bayesian_4_~~Cor~~OHcor and the Bayesian_4_~~Cor_F.~~

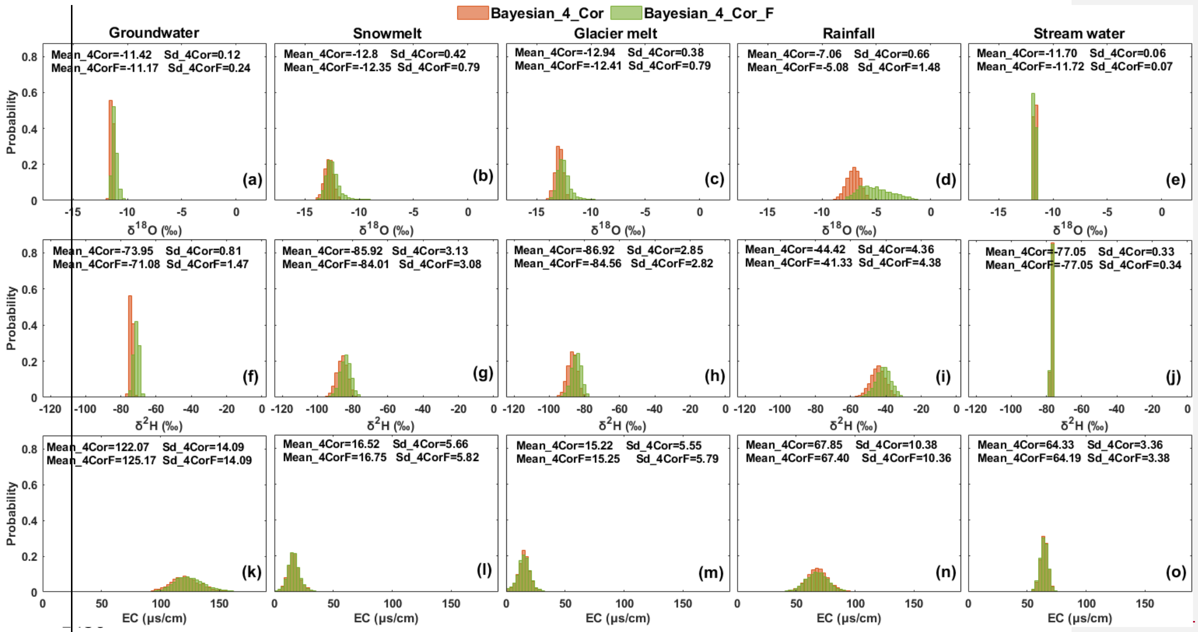

1437 OHcor_Frac.

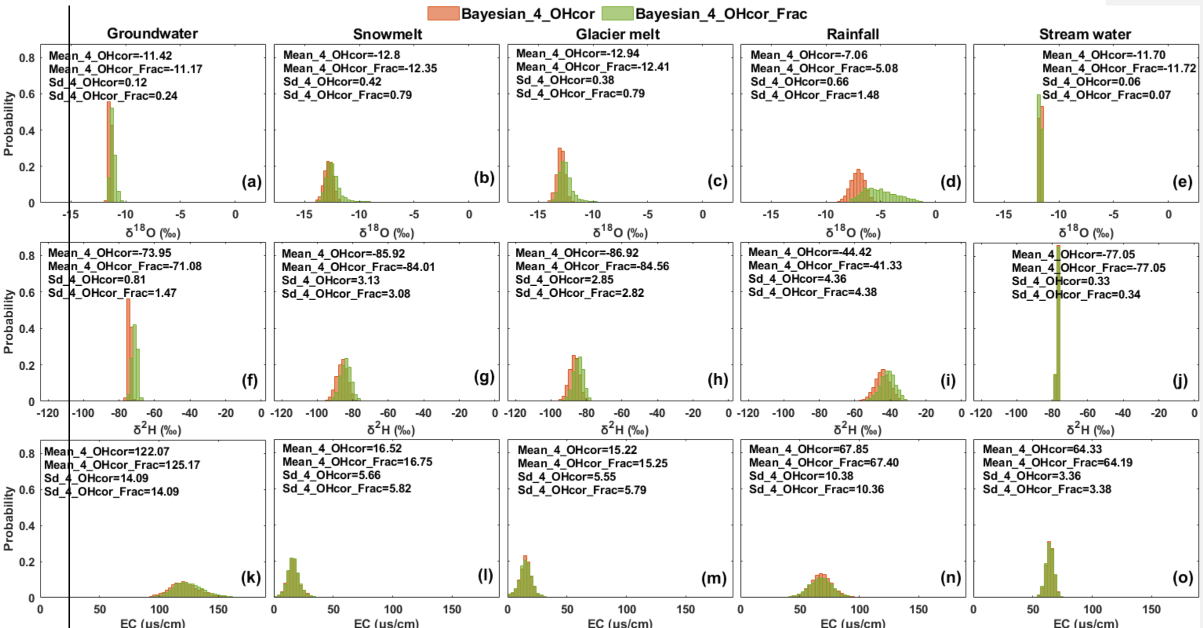

Figure 10. Effects of isotope fractionation on the posterior distributions of tracer signatures of water sources in the glacier melt season.